

# Probabilistic Filtered Soft Labels for Domain Adaptation

Wei Wang, Zhihui Wang\*, Haojie Li, and Zhengming Ding

**Abstract**—Many domain adaptation (DA) methods aim to project the source and target domains into a common feature space, where the inter-domain distributional differences are reduced and some intra-domain properties preserved. Recent research obtains their respective new representations using some predefined statistics. However, they usually formulate the class-wise statistics using the pseudo hard labels due to no labeled target data, such as class-wise MMD and class scatter matrix. The probabilities of data points belonging to each class given by the hard labels are either 0 or 1, while the soft labels could relax the strong constraint of hard labels and provide a random value between them. Although existing work have noticed the advantage of soft labels, they either deal with those class-wise statistics inadequately or introduce those small irrelevant probabilities in soft labels. Therefore, we propose the filtered soft labels to discard those confusing probabilities, then both of the class-wise MMD and class scatter matrix are modeled in this way. In order to obtain more accurate filtered soft labels, we take advantage of a well-designed Graph-based Label Propagation (GLP) method, and incorporate it into the DA procedure to formulate a unified framework. Specifically, the graph in GLP is updated using the transferred features, then the predictive filtered soft labels are utilized to model the class-wise statistics in DA. It is remarkable that the adopted GLP method could discover novel classes by adding an extra component into the predictive label vectors, thus it could be easily extended to open set DA scenario, which allows the target domain contains unknown classes that are not observed in the source domain. Therefore, the probabilities of a data instance belonging to the common or novel classes could be obtained, then the positive knowledge transfer between common classes of each domain could be realized, where the novel classes are suppressed using the smaller probabilistic weights. Comprehensive experiments on benchmark cross-domain object recognition datasets verify that our approach outperforms several state-of-the-art methods.

**Index Terms**—Domain adaptation, close set domain adaptation, open set domain adaptation, label propagation, probabilistic filtered soft labels.

## I. INTRODUCTION

**T**RADITIONAL machine learning algorithms always assume that the training and test data are drawn from the same distribution. Unfortunately, this assumption could not hold on account of the complicated practical applications [1]. For example, in visual recognition, the distributions of training and test can be different due to the environments, sensor types, resolutions and view angles. Since relabeling new target domain data is time-consuming and labor-intensive, it is impractical to relabel a large amount of data in a new domain. Fortunately, the Domain Adaptation (DA) [2], [3], [4] has been proposed to address these challenges. The goal of DA is to employ previous labeled source domain data to boost the task in the new target domain. It is widely applied

to cross-domain data mining for reusing labeled information and mitigating labeling consumption.

The most popular DA technique is the Feature-based DA (FDA) [5], [6], [7], which projects different domains data into a shared subspace or their respective subspaces with inter-domain distribution differences reduced largely or intra-domain properties preserved maximumly, then the classifier trained on the source domain could be easily applied to the target domain. For this purpose, Pan *et al.* [8] proposed the Transfer Component Analysis (TCA) to match the marginal distributions between different domains in Reproducing Kernel Hilbert Space (RKHS) using the Maximum Mean Discrepancy (MMD). Long *et al.* [36] aimed to refine the latent factors to alleviate negative transfer by preserving the intra-domain geometric structure.

Due to importance of the class-wise information, Long *et al.* [7] improved TCA to align the marginal distributions for the same classes from different domains using the class-wise MMD, thus the difference in conditional distributions decreases. Some remarkable approaches took aim at preserving the discriminative information of either source or target domains using the class scatter matrix, such as DICD (Domain Invariant and Class Discriminative Feature Learning) [5], VDA (Visual Domain Adaptation) [9], SCA (Scatter Component Analysis) [10], JGSA (Joint Geometrical and Statistical Alignment) [6].

Existing research confirmed that the DA performance is mainly determined by those class-wise information, thus how to model them as correctly as possible is a key factor in despite of no labeled target data. However, most of FDA methods usually formulate the class-wise statistics using the target pseudo hard labels, such as class-wise MMD and class scatter matrix. The probabilities of data points belonging to each class given by the hard labels are either 0 or 1. This could hurt the knowledge transfer since target samples might be predicted wrongly in the beginning. Moreover, when target samples from two classes have overlap distribution, it would easily undermine the intrinsic structure within the data by assigning only one hard label to those samples.

What is different is that the soft labels provide a random value between 0 and 1 for those probabilities, which offers the possibility for reformulating those class-wise statistics in DA and alleviates the negative transfer incurred by the hard labels. In this regard, Ding *et al.* [11] introduced a probabilistic class-wise MMD for inter-domain distributional alignment (Graph Adaptive Knowledge Transfer, GAKT), while they did not further consider the intra-domain discriminative information in this probabilistic way. Besides, the small irrelevant proba-

bilities in soft labels were not filtered out which were confusing so that their model would be unstable. This mainly may be stemmed from the following reason: when a data instance just hesitates in several classes or definitely belongs to one class, it is apparent that taking those probabilities all into account will introduce so much noise.

Different from them, this paper proposes a probabilistic filtered soft labels to reformulate the class-wise MMD and class scatter matrices simultaneously for positive knowledge transfer, and sufficient consideration of the discriminative information is given in the source and target domains. Specifically, we filter out the small probabilities in soft labels to ensure that the soft labels are as sparse as possible. Moreover, we take advantage of the graph-based label propagation (GLP) [12] and incorporate it into the DA procedure, where the graph is updated with the transferred features in DA for more accurate filtered soft labels, then the filtered soft labels based class-wise statistics could facilitate more positive knowledge transfer.

Another challenge is that the Open Set Domain Adaptation (OSDA) [14], [15], [16], which relaxes the assumption that the source and target domains share the same label space in Closed Set Domain Adaptation (CSDA) [13]. The OSDA is a more realistic setting, since we cannot decide whether source and target domains share the same label space if no target annotations are available. The most critical issue in OSDA is how to correctly discover the novel classes in the target domain, then realize knowledge transfer only between the common classes. In this paper, we mainly follow the setting from Saito et al. [15] and Liu et al. [16], where the target domain has all classes in the source domain and further contains target-specific classes.

Although GAKT first proposed to jointly model knowledge transfer and label propagation in a unified framework, the label propagation in their model failed to discover the novel classes. Different from them, we incorporate a general graph-based label propagation with novel class discovery [12] into the DA framework, where an additional component is embedding into the vectors of predictive soft labels in order to capture the unknown classes in the target domain. Then the proposed model could be easily extended to deal with the OSDA setting, and the correct knowledge between the two domains could be transferred, where the data instances of common classes are assigned with larger probabilistic weights than those unknown classes in the target domain.

The main contributions of our work are three-folds:

- We simultaneously reformulate the class-wise MMD and class scatter matrices using the filtered soft labels, so that the strong constraint of hard labels could be relaxed and the noise irrelevant probabilities in soft labels are discarded.
- A general model are proposed which merge the GLP with DA procedures so that the filtered soft labels are more accurate, where the graph in GLP is updated by the transferred features in DA.
- The proposed model could be easily extended to deal with the OSDA problem, where the common knowledge between two domains could be transferred correctly in a probabilistic weight mechanism.

The remainder of this paper is organized as follows. In Section II, we review the related work in DA. In Section III, we introduce the proposed PFSLG-DA approach for challenges of CSDA and OSDA, and its optimization procedure. In Section IV, the experiments in cross-domain visual recognition are presented. Finally, the paper is concluded in Section V.

## II. RELATED WORK

Domain Adaptation (DA) aims to generalize the classifier learned from the source domain to the target domain [17], [18]. Recent DA methods follow a mainstream approach called the Feature-based Domain Adaptation (FDA), which integrates with certain feature extraction methods for discovering projections to map different domains data into a common feature subspace, where the distances of marginal and conditional distributions between domains decrease. Taking different feature extraction methods into account, FDA will fall into two main categories, namely the shallow FDA methods and the Deep FDA methods [19]. The most representative examples are the recent trends in Deep Neural Networks-based FDA [20], [21], [22] and Generative Adversarial Networks-based FDA [23], [24], [25], [26] which has shown great improvements in the performance of adaptive features due to the available substantial amount of labeled data. However, due to the inherent bias within different datasets [27], [28], using a large amount of labeled training data does not warrant a better performance by these models [29]. Moreover, most of them have learned a transfer network to align the distribution of layers by embedding some criteria from the shallow FDA methods, *e.g.*, DAN [30], JAN [31]. Therefore, the research of the shallow FDA is very urgent and significant, which can be regarded as a transferable layer and is instructive for network design. Although the proposed method is a shallow FDA paradigm, the competitive capability comparing to those Deep FDA methods has been validated on the pre-extracted deep features.

Numerous shallow FDA approaches have been proposed using different feature extraction algorithms in the past few years. As an unsupervised feature learning algorithm, PCA (Principal Component Analysis) is applied to extract the common features in DA due to the simpler procedure of matrix optimization. For example, in order to construct new feature representation that is invariant to both the distributional difference and the irrelevant instances, TJM [32] was proposed to reduce the domain difference by jointly matching the features and reweighting the instances across domains in PCA. Furthermore, Wang *et al.* [33] proposed Balanced Distribution Adaptation (BDA) to adaptively leverage the importance of the marginal and conditional distribution discrepancies in PCA. After that, the sparse coding has received more attention in many research fields, which makes the representation more succinct and easy to manipulate. Therefore, Long *et al.* [34] incorporated sparse coding into DA to make the new representation robust to the distributional difference. Zhang *et al.* [35] proposed a latent sparse domain transfer (LSDT) for domain adaptation and visual categorization of heterogeneous data. As another effective approach of feature extraction, the

NMF (Non-negative Matrix Factorization) has received considerable attention due to its psychological and physiological interpretation of naturally occurring data whose representation may be parts-based in the human brain. Hence, Long *et al.* [36] proposed a Graph Co-Regularized Transfer Learning (GTL), which used NMF to extract common latent factors for knowledge transfer. Ievgen *et al.* [37] proposed a Random Subspaces NMF for unsupervised transfer learning. Wang *et al.* [38] proposed the domain transfer NMF approach for data representation. Recently, most representative approaches exploit the common subspace in DA via a low-rank representation method, which attempts to minimize the discrepancy between the source data and target data so that the data in the source domain can be linearly represented by the data in the target domain. Jhuo *et al.* [39] presented a low-rank reconstruction method to reduce the domain distribution disparity, which transforms the visual samples in the source domain to an intermediate representation such that each transformed source sample can be linearly reconstructed by the samples of the target domain. Shao *et al.* [40] utilized the low-rank constraint to bridge the source and the target domain in the low-dimensional space for transfer subspace learning. Zhang *et al.* [19] proposed a manifold criterion guided transfer learning method, which generated an intermediate domain using low-rank constraint to connect the source and the target domains effectively. In order to highlight the contributions in this paper and make the model more simpler, we realize the knowledge transfer in PCA framework.

Most of the aforementioned methods only pursue minimizing the inter-domain distributional differences, which can be achieved by explicitly minimizing predefined distance metrics, *e.g.*, Bregman Divergence [41], Geodesic Distance [42] and Maximum Mean Discrepancy (MMD) [43]. The most popular distance is MMD due to its simplicity and solid theoretical foundations. However, the disparity in distributions between different domains is not the only factor affecting the cross-domain visual recognition, but also some intra-domain data properties. Therefore, LRSR [44] and DLC [45] were proposed to lessen the classification errors in the source domain. As a significant domain specific property, discriminative information preservation enforces the distances of embedded representations from the same classes smaller, while the distances of embedded representations from different classes larger [46]. Therefore, some classical methods, such as and DICD [5], VDA [9] and SCA [10], were proposed to construct the class scatter matrix to preserve the discriminative information of each domain. However, they only exploit invariant features and structures in a shared subspace, which will fail when the two different domains have large discrepancy, because there may not exist such a common space where the distributions of two domains are the same and the data properties are also maximumly preserved in the mean time. Based on this, some subspace centric approaches were proposed to address this issue, such as GFK [42], SA [47], SDA [48]. Furthermore, Zhang *et al.* [6] proposed Joint Geometrical and Statistical Alignment (JGSA) using two coupled projections, then the relative importance of inter-domain differences and intra-domain properties could be adapted by regulating how close the source

subspace is to the target one. Another difficulty is that most class-wise statistics in previous models are formulated by the target pseudo hard labels since there are no target labeled data instances, while the experimental results in this paper show that the hard labels are too absolute to positive transfer. Although the recent work GAKT [11] aimed to deal with this problem using a probabilistic class-wise MMD, they did not further consider the intra-domain discriminative information and the OSDA challenge in this probabilistic mechanism, and did not filter out the small probabilities in soft labels which might confuse the stability of their model.

Recently, Open Set Domain Adaptation (OSDA) as a novel DA setting arouses researchers' widespread concern [13], [14], [15], [16], which relaxes the strong assumption in CSDA and allows the target domain to contain some unknown classes that are absent in the source domain. Actually, OSDA is more practical, especially for the "in-the-wild" setting where we cannot constrain the boundary of classes in the target domain. Specifically, OSDA mainly introduces two challenges. 1) It is still essential to mitigate the influence of distributional shift between domains as CSDA did. 2) In addition, aligning the whole distributions of source and target domains as before will be risky since data of unknown classes in the target domain can make performance of DA model even inferior to a model without adaptation. Such phenomenon is known as negative transfer [1]. Thus, in OSDA setting, we need to identify the boundary between known and unknown classes as accurately as possible, even without accessible information about the unknown classes. We should further apply adaptation to the known classes in both domains.

Different from them, in this paper, we utilize the probabilistic filtered soft labels to reformulate both the class-wise MMD and class scatter matrix, where the small probabilities in soft labels are filtered out. Moreover, a well-designed GLP method is incorporated into DA procedure, where the graph is updating by the transferred features in DA. As for OSDA problem, only a few approaches are proposed and most of them belong to the Deep FDA methods. Different from them, in this paper, a shallow FDA method is proposed to capture the unknown classes in the target domain, then the knowledge transfer could be realized between the common classes of each domain.

### III. PROBABILISTIC SOFT LABELS GUIDED DOMAIN ADAPTATION

#### A. Preliminaries

Given a labeled source domain  $D_s$  (the number of samples is  $n_s$ ), *i.e.*,  $D_s = \{(\mathbf{x}_1, \mathbf{y}_1), \dots, (\mathbf{x}_{n_s}, \mathbf{y}_{n_s})\}$ , while an unlabeled target domain  $D_t$  (the number of samples is  $n_t$ ), *i.e.*,  $D_t = \{\mathbf{x}_{n_s+1}, \dots, \mathbf{x}_{n_s+n_t}\}$ . Assuming that the feature space  $\Omega_s = \Omega_t$ , while the marginal distribution  $P_s(\mathbf{x}_s) \neq P_t(\mathbf{x}_t)$  and conditional distribution  $Q_s(\mathbf{y}_s|\mathbf{x}_s) \neq Q_t(\mathbf{y}_t|\mathbf{x}_t)$  (*i.e.*, the labeling functions  $\mathbf{f}_s(\mathbf{x}_s), \mathbf{f}_t(\mathbf{x}_t)$ ), we aim to find projections  $\mathbf{A}$  and  $\mathbf{B}$  to map  $D_s$  and  $D_t$  into their respective subspaces where the distributional differences between them (*i.e.*,  $P_s(\mathbf{x}_s)$  and  $P_t(\mathbf{x}_t)$ ,  $Q_s(\mathbf{y}_s|\mathbf{x}_s)$  and  $Q_t(\mathbf{y}_t|\mathbf{x}_t)$ ) are explicitly reduced ( $\mathbf{A} = \mathbf{B}$  or  $\mathbf{A} \approx \mathbf{B}$ ). As mentioned above, the CSDA setting is that the label space  $\Upsilon_s = \Upsilon_t$  while the OSDA  $\Upsilon_s \subset \Upsilon_t$ .

For the convenience of matrix calculus, we represent the source and target data as a data matrix respectively, *i.e.*,  $\mathbf{X}_s \in \mathbf{R}^{m \times n_s}$ ,  $\mathbf{X}_t \in \mathbf{R}^{m \times n_t}$ , where  $m$  is the feature dimension. The whole data matrix is  $\mathbf{X} = [\mathbf{X}_s, \mathbf{X}_t] \in \mathbf{R}^{m \times n}$  and it is centered in advance, where  $n = n_s + n_t$ . For leveraging the domain-specific subspaces, we define two projections  $\mathbf{A}, \mathbf{B} \in \mathbf{R}^{m \times k}$ , the new data representation  $\mathbf{Z}_s = \mathbf{A}^T \mathbf{X}_s$ ,  $\mathbf{Z}_t = \mathbf{B}^T \mathbf{X}_t$ , ( $\mathbf{Z}_s \in \mathbf{R}^{k \times n_s}$ ,  $\mathbf{Z}_t \in \mathbf{R}^{k \times n_t}$ ), and the dimension is  $k$  ( $k \ll m$ ).

### B. Probabilistic Soft Labels Guided Domain Adaptation

As mentioned before, the inter-domain distributional alignment and intra-domain data properties preservation are of equal importance for the final DA performance. Moreover, there may not exist such a common space where those two issues are optimized effectively in the mean time. Therefore, we propose to consider them using two coupled projections ( $\mathbf{A} \approx \mathbf{B}$ ), and formulate it as follows:

$$\max \frac{(\text{dist})_{\text{inter}}^s + (\text{dist})_{\text{inter}}^t}{(\text{dist})_{\text{intra}}^s + (\text{dist})_{\text{intra}}^t + (\text{shift})_{\text{domain}} + (\text{shift})_{\text{subspace}}}, \quad (1)$$

where we maximize the distances of the embedded representations from different classes (*i.e.*,  $(\text{dist})_{\text{inter}}^s$  for source domain and  $(\text{dist})_{\text{inter}}^t$  for target domain), while minimize the distances of the embedded representations from the same classes (*i.e.*,  $(\text{dist})_{\text{intra}}^s$  and  $(\text{dist})_{\text{intra}}^t$ ). In addition, the distributional shift and the subspace shift should be reduced by  $(\text{shift})_{\text{domain}}$  and  $(\text{shift})_{\text{subspace}}$  terms.

In order to model  $(\text{dist})_{\text{inter}}^s$ ,  $(\text{dist})_{\text{inter}}^t$ ,  $(\text{dist})_{\text{intra}}^s$ ,  $(\text{dist})_{\text{intra}}^t$  effectively, we have to construct the inter-class and intra-class scatter matrix (*i.e.*,  $\mathbf{S}_b$  and  $\mathbf{S}_w$ ), while they belong to class-wise statistics and require accurate data annotations. Unfortunately, the target domain data are unlabeled in the unsupervised DA scenario. Most previous methods aimed to model them utilizing the target pseudo hard labels, while our experimental results showed that the hard labels might be too absolute to positive transfer. Different from them, we reformulate them using all samples with given probabilities (soft labels) but not just one specific class. The soft labels are defined as  $\mathbf{F} \in \mathbf{R}^{n \times C}$ , (*e.g.*, the probability  $F_{ic}$  of  $\mathbf{x}_i$  belonging to class  $c$ ,  $c \in \{1 \dots C\}$ ). While the original  $\mathbf{S}_b$  and  $\mathbf{S}_w$  are based on the hard labels, (*e.g.*, the probability  $F_{ic}$  of  $\mathbf{x}_i$  belonging to class  $c$  is either 0 or 1). We formulate the soft labels-based scatter matrix (*i.e.*,  $\mathbf{S}_b, \mathbf{S}_w$ ) as follows:

$$\mathbf{S}_b = \sum_{i=1}^C \frac{\tilde{n}^{(i)}}{n} (\tilde{\mathbf{x}}^{(i)} - \tilde{\mathbf{x}})(\tilde{\mathbf{x}}^{(i)} - \tilde{\mathbf{x}})^T \quad (2)$$

$$= \frac{1}{n} \mathbf{X}(\mathbf{F}\mathbf{K}\mathbf{F}^T - \frac{1}{n} \mathbf{B}\mathbf{I}\mathbf{I}^T \mathbf{B})\mathbf{X}^T,$$

$$\mathbf{S}_w = \frac{1}{n} \sum_{i=1}^C \sum_{j=1}^n \mathbf{F}_{ji} (\mathbf{x}_j - \tilde{\mathbf{x}}^{(i)})(\mathbf{x}_j - \tilde{\mathbf{x}}^{(i)})^T \quad (3)$$

$$= \frac{1}{n} \mathbf{X}(\mathbf{B} - \mathbf{F}\mathbf{K}\mathbf{F}^T)\mathbf{X}^T,$$

where  $\tilde{n}^{(i)} = \sum_{j=1}^n \mathbf{F}_{ji}$ ,  $\tilde{n} = \sum_{i=1}^C \tilde{n}^{(i)}$ ,  $\tilde{\mathbf{x}}^{(i)} = \sum_{j=1}^n \mathbf{F}_{ji} \mathbf{x}_j / \tilde{n}^{(i)}$ ,  $\tilde{\mathbf{x}} = \sum_{j=1}^n \sum_{i=1}^C \mathbf{F}_{ji} \mathbf{x}_j / \tilde{n}$ ,  $\mathbf{B} \in \mathbf{R}^{n \times n}$  is a diagonal matrix, the  $j$ -th diagonal element of which is  $\mathbf{B}_{jj} = \sum_{i=1}^C \mathbf{F}_{ji}$ ,  $\mathbf{K} \in \mathbf{R}^{C \times C}$  is a diagonal matrix,

the  $i$ -th diagonal element of which is  $\mathbf{K}_{ii} = 1 / \sum_{j=1}^n \mathbf{F}_{ji}$ ,  $\mathbf{I} = [1, \dots, 1]^T \in \mathbf{R}^{n \times 1}$ . When the soft labels become hard ones, it can be easily checked that the soft labels-based scatter matrix defined here become the hard labels-based ones. One can note that, the statistics for each class are computed not using the samples from one specific class, but the whole samples weighted by the probabilities belonging to this class. Moreover, we noticed that the small probabilities in soft labels also have a bad effect on positive transfer, thus we discard them so that one sample only hesitates in several classes. Finally, this probabilistic filtered soft labels guided mechanism could alleviate the negative transfer to some degree.

As for  $(\text{shift})_{\text{domain}}$  across two different domains, it could be divided into the marginal distribution shift and conditional distribution shift. Firstly, we utilize the Maximum Mean Discrepancy (MMD), which is an effective distance-measure method with non-parameter, to compare the marginal distributions of two data sets by matching each statistical moment of them. For simplicity, we compute the deviation between the means (*i.e.*, first-order moment) of the source and target domains in the Euclidean space, so as to explicitly minimize their marginal distribution difference in the new embedded subspaces (*i.e.*,  $\mathbf{Z}_s, \mathbf{Z}_t$ ), and the formula is as follows:

$$\begin{aligned} & \left\| \frac{1}{n_s} \sum_{i=1}^{n_s} \mathbf{A}^T \mathbf{x}_i - \frac{1}{n_t} \sum_{j=n_s+1}^{n_s+n_t} \mathbf{B}^T \mathbf{x}_j \right\|^2 \\ &= \text{tr} \left( \begin{bmatrix} \mathbf{A}^T & \mathbf{B}^T \end{bmatrix} \begin{bmatrix} \mathbf{M}_s^{(0)} & \mathbf{M}_{st}^{(0)} \\ \mathbf{M}_{ts}^{(0)} & \mathbf{M}_t^{(0)} \end{bmatrix} \begin{bmatrix} \mathbf{A} \\ \mathbf{B} \end{bmatrix} \right), \end{aligned} \quad (4)$$

where  $\mathbf{M}_s^{(0)}, \mathbf{M}_{st}^{(0)}, \mathbf{M}_t^{(0)}, \mathbf{M}_{ts}^{(0)}$  are the MMD matrix. We define the matrix  $\mathbf{I}_s = [1, \dots, 1]^T \in \mathbf{R}^{n_s \times 1}$  and  $\mathbf{I}_t = [1, \dots, 1]^T \in \mathbf{R}^{n_t \times 1}$ , then the MMD matrix are computed as follows:

$$\mathbf{M}_s^{(0)} = \mathbf{X}_s \mathbf{I}_s^{(0)} \mathbf{X}_s^T, \quad \mathbf{I}_s^{(0)} = \frac{1}{n_s^2} \mathbf{I}_s \mathbf{I}_s^T, \quad (5)$$

$$\mathbf{M}_t^{(0)} = \mathbf{X}_t \mathbf{I}_t^{(0)} \mathbf{X}_t^T, \quad \mathbf{I}_t^{(0)} = \frac{1}{n_t^2} \mathbf{I}_t \mathbf{I}_t^T, \quad (6)$$

$$\mathbf{M}_{st}^{(0)} = \mathbf{X}_s \mathbf{I}_{st}^{(0)} \mathbf{X}_t^T, \quad \mathbf{I}_{st}^{(0)} = -\frac{1}{n_s n_t} \mathbf{I}_s \mathbf{I}_t^T, \quad (7)$$

$$\mathbf{M}_{ts}^{(0)} = \mathbf{X}_t \mathbf{I}_{ts}^{(0)} \mathbf{X}_s^T, \quad \mathbf{I}_{ts}^{(0)} = -\frac{1}{n_s n_t} \mathbf{I}_t \mathbf{I}_s^T, \quad (8)$$

With regard to the conditional distribution  $Q(\mathbf{y}|\mathbf{x})$ , since the posterior probabilities  $Q_s(\mathbf{y}_s|\mathbf{x}_s)$  and  $Q_t(\mathbf{y}_t|\mathbf{x}_t)$  are quite involved, we resort to explore the sufficient statistics of class-wise distributions  $Q_s(\mathbf{x}_s|\mathbf{y}_s)$  and  $Q_t(\mathbf{x}_t|\mathbf{y}_t)$  instead [7]. Then we match the first-order moments for the same class from  $D_s$  and  $D_t$  in the Euclidean space, *i.e.*, the MMD distance between the distributions of  $Q_s(\mathbf{x}_s|\mathbf{y}_s = c)$  and  $Q_t(\mathbf{x}_t|\mathbf{y}_t = c)$ , called class-wise MMD. Similarly, the class-wise MMD could be reformulated utilizing the soft labels and the formula is as follows:

$$\begin{aligned} & \sum_{i=1}^C \left\| \frac{1}{\tilde{n}_s^{(i)}} \sum_{j=1}^{n_s} \mathbf{F}_{ji} \mathbf{A}^T \mathbf{x}_j - \frac{1}{\tilde{n}_t^{(i)}} \sum_{j=n_s+1}^{n_s+n_t} \mathbf{F}_{ji} \mathbf{B}^T \mathbf{x}_j \right\|^2 \\ &= \sum_{i=1}^C \text{tr} \left( \begin{bmatrix} \mathbf{A}^T & \mathbf{B}^T \end{bmatrix} \begin{bmatrix} \mathbf{M}_s^{(i)} & \mathbf{M}_{st}^{(i)} \\ \mathbf{M}_{ts}^{(i)} & \mathbf{M}_t^{(i)} \end{bmatrix} \begin{bmatrix} \mathbf{A} \\ \mathbf{B} \end{bmatrix} \right), \end{aligned} \quad (9)$$

where  $\tilde{n}_s^{(i)} = \sum_{j=1}^{n_s} \mathbf{F}_{ji}$ ,  $\tilde{n}_t^{(i)} = \sum_{j=n_s+1}^{n_s+n_t} \mathbf{F}_{ji}$ ,  $\mathbf{M}_s^{(i)}, \mathbf{M}_{st}^{(i)}, \mathbf{M}_t^{(i)}, \mathbf{M}_{ts}^{(i)}$  are the class-wise MMD matrice, and they are computed as follows:

$$\begin{aligned} \mathbf{M}_s^{(i)} &= \mathbf{X}_s \mathbf{L}_s^{(i)} \mathbf{X}_s^T, \quad \mathbf{L}_s^{(i)} = \mathbf{F}_s^{(i)} \bullet \mathbf{e}_s^{(i)} \bullet \mathbf{e}_s^{(i)T} \bullet \mathbf{F}_s^{(i)} \\ \mathbf{F}_s^{(i)} &= \text{diag}(\mathbf{F}(1:n_s, i)), \end{aligned} \quad (10)$$

$$\begin{aligned} \mathbf{e}_s^{(i)}(1:n_s) &= 1 / \sum_{j=1}^{n_s} \mathbf{F}(j, i), \quad \mathbf{e}_s^{(i)} \in \mathbf{R}^{n_s \times 1} \\ \mathbf{M}_t^{(i)} &= \mathbf{X}_t \mathbf{L}_t^{(i)} \mathbf{X}_t^T, \quad \mathbf{L}_t^{(i)} = \mathbf{F}_t^{(i)} \bullet \mathbf{e}_t^{(i)} \bullet \mathbf{e}_t^{(i)T} \bullet \mathbf{F}_t^{(i)} \\ \mathbf{F}_t^{(i)} &= \text{diag}(\mathbf{F}(n_s+1:n, i)), \end{aligned} \quad (11)$$

$$\begin{aligned} \mathbf{e}_t^{(i)}(1:n_t) &= -1 / \sum_{j=n_s+1}^n \mathbf{F}(j, i), \quad \mathbf{e}_t^{(i)} \in \mathbf{R}^{n_t \times 1} \\ \mathbf{M}_{st}^{(i)} &= \mathbf{X}_s \mathbf{L}_{st}^{(i)} \mathbf{X}_t^T, \quad \mathbf{L}_{st}^{(i)} = \mathbf{F}_s^{(i)} \bullet \mathbf{e}_s^{(i)} \bullet \mathbf{e}_t^{(i)T} \bullet \mathbf{F}_t^{(i)} \end{aligned} \quad (12)$$

$$\mathbf{M}_{ts}^{(i)} = \mathbf{X}_t \mathbf{L}_{ts}^{(i)} \mathbf{X}_s^T, \quad \mathbf{L}_{ts}^{(i)} = \mathbf{F}_t^{(i)} \bullet \mathbf{e}_t^{(i)} \bullet \mathbf{e}_s^{(i)T} \bullet \mathbf{F}_s^{(i)} \quad (13)$$

Concerning the subspaces shift between the two domains, we use following term to move them close:

$$\min_{\mathbf{A}, \mathbf{B}} \|\mathbf{A} - \mathbf{B}\|_F^2, \quad (14)$$

and we follow [6] to further impose the constraint that  $\gamma \text{Tr}(\mathbf{A}^T \mathbf{A})$  and  $\gamma \text{Tr}(\mathbf{B}^T \mathbf{B})$  are small to control the scale of  $\mathbf{A}$  and  $\mathbf{B}$ . Moreover, it can be verified that the variance matrix  $\mathbf{S}_t = \mathbf{S}_w + \mathbf{S}_b$  [49], thus we optimize  $(\mathbf{dist})_{\text{inter}}^s$  and  $(\mathbf{dist})_{\text{inter}}^t$  using  $\mathbf{S}_t^{(s)}$  and  $\mathbf{S}_t^{(t)}$  instead for simplicity. Finally, we incorporate the quantities defined above into Eq. (1) as follows:

$$\max_{\mathbf{A}, \mathbf{B}} \frac{\text{tr} \left( \begin{bmatrix} \mathbf{A}^T & \mathbf{B}^T \end{bmatrix} \begin{bmatrix} \mathbf{S}_t^{(s)} & \mathbf{0} \\ \mathbf{0} & \mathbf{S}_t^{(t)} \end{bmatrix} \begin{bmatrix} \mathbf{A} \\ \mathbf{B} \end{bmatrix} \right)}{\sum_{i=0}^C \text{tr} \left( \begin{bmatrix} \mathbf{A}^T & \mathbf{B}^T \end{bmatrix} \begin{bmatrix} \mathbf{ST}_1^{(i)} & \mathbf{ST}_2^{(i)} \\ \mathbf{ST}_3^{(i)} & \mathbf{ST}_4^{(i)} \end{bmatrix} \begin{bmatrix} \mathbf{A} \\ \mathbf{B} \end{bmatrix} \right)}, \quad (15)$$

$$\begin{aligned} \mathbf{ST}_1^{(i)} &= \delta \mathbf{M}_s^{(i)} + (\lambda + \gamma) \mathbf{I}_m + \gamma_{st} \mathbf{S}_w^{(s)}, \\ \mathbf{ST}_2^{(i)} &= \delta \mathbf{M}_{st}^{(i)} - \lambda \mathbf{I}_m, \\ \mathbf{ST}_3^{(i)} &= \delta \mathbf{M}_{ts}^{(i)} - \lambda \mathbf{I}_m, \\ \mathbf{ST}_4^{(i)} &= \delta \mathbf{M}_t^{(i)} + (\lambda + \gamma) \mathbf{I}_m + \gamma_{st} \mathbf{S}_w^{(t)}, \end{aligned} \quad (16)$$

where  $\delta, \lambda, \gamma, \gamma_{st}$  are trade-off parameters to balance the importance of each quantity, and  $\mathbf{I}_m \in \mathbf{R}^{m \times m}$  is an identify matrix.

One intuitive question is that how to feed more accurate soft labels to Eq. (15), we take advantage of the graph-based label propagation (GLP) method [12], [49] and merge it with the DA procedure. As a semi-supervised learning algorithm, GLP aims to propagate label information from labeled data to unlabeled data according to the distribution of labeled and unlabeled data, where the probabilities of the unlabeled points belonging to each class could be obtained (*i.e.*, soft labels). In the GLP, a neighborhood weighted graph on data should be constructed first. A popular construction method is as follows: if  $\mathbf{x}_i$  is among the  $p$ -nearest neighbors of  $\mathbf{x}_j$  or  $\mathbf{x}_j$  is among the  $p$ -nearest neighbors of  $\mathbf{x}_i$ , then  $\mathbf{x}_i$  and  $\mathbf{x}_j$  are linked by a weight computed by:  $\mathbf{W}_{ij} = e^{-\|\mathbf{x}_i - \mathbf{x}_j\|^2 / \sigma^2}$ , otherwise,  $\mathbf{W}_{ij} = 0$ . Here  $\sigma$  is the variance. The GLP procedure can be formulated as follows:

$$\min_{\mathbf{F}} \sum_{i,j=1}^n \mathbf{W}_{ij} \|\mathbf{F}_i - \mathbf{F}_j\|_F^2 + \sum_{i=1}^n \mu_i h_i \|\mathbf{F}_i - \mathbf{Y}_i\|_F^2, \quad (17)$$

where  $\mu_i$  is a regularization parameter for each data  $\mathbf{x}_i$  and the soft label  $\mathbf{F}_i$  is the row vector and each element belongs to  $[0,1]$ . The matrix  $\mathbf{Y} = [\mathbf{Y}_1, \dots, \mathbf{Y}_n] \in \mathbf{R}^{n \times C}$ , ( $\mathbf{Y}_{ij} = 1$  if  $\mathbf{x}_i$  is labeled as  $j$  and  $\mathbf{Y}_{ij} = 0$  otherwise for the source domain, while each element of  $\mathbf{Y}_i$  is 0 for the target domain), and  $h_i = \sum_j \mathbf{W}_{ij}$ .

Therefore, we incorporate Eq. (17) into Eq. (15) and obtain our final learning objective for CSDA as follows:

$$\begin{aligned} & \max_{\mathbf{Q}} \text{tr} \left( \mathbf{Q}^T \begin{bmatrix} \mathbf{S}_t^{(s)} & \mathbf{0} \\ \mathbf{0} & \mathbf{S}_t^{(t)} \end{bmatrix} \mathbf{Q} \right) - \text{tr}(\mathbf{F}^T \mathbf{L} \mathbf{F}) \\ & \quad - \text{tr}((\mathbf{F} - \mathbf{Y})^T \mathbf{U} \mathbf{H} (\mathbf{F} - \mathbf{Y})) \end{aligned} \quad (18)$$

$$\text{s.t.} \quad \sum_{i=0}^C \text{tr} \left( \mathbf{Q}^T \begin{bmatrix} \widetilde{\mathbf{ST}}_1^{(i)} & \widetilde{\mathbf{ST}}_2^{(i)} \\ \widetilde{\mathbf{ST}}_3^{(i)} & \widetilde{\mathbf{ST}}_4^{(i)} \end{bmatrix} \mathbf{Q} \right) = 1,$$

where  $\mathbf{Q}^T = [\mathbf{A}^T \quad \mathbf{B}^T]$ , and  $\mathbf{H}, \mathbf{U} \in \mathbf{R}^{n \times n}$  are diagonal matrices (*i.e.*,  $\mathbf{H}_{ii} = h_i, \mathbf{U}_{ii} = \mu_i$ ), and  $\mathbf{L} = \mathbf{H} - \mathbf{W}$ . It is a novel FDA model with jointly inter-domain distributional alignment and intra-domain discriminative preservation. Specifically, the soft labels predicted by GLP are utilized to reformulate the class-wise MMD and class scatter matrice, and the transferred features are exploited to update the neighborhood weighted graph to improve the quality of soft labels.

With respect to the classification errors in the source domain, it could be reduced greatly by adjusting the parameter  $\mu_i$  in Eq. (18). Let us introduce a set of variables  $\alpha_i = 1/(1 + \mu_i)$ , ( $i = 1, \dots, n$ ), while  $\beta_i = 1 - \alpha_i$ , ( $i = 1, \dots, n$ ). The label information of each data is partly received from its neighbors' labels, and the rest is received from its initial label  $\mathbf{y}_i$ . Usually, for the data point from source domain, we are sure that the initial label is definitely correct,  $\alpha_i$  can be set to zero, which means the resulted label of  $\mathbf{x}_i$  will be equal to the initial label and remains unchanged. Thus, the classification

errors in the source domain could be reduced to zero. For the data point from target domain,  $\alpha_i$  can be set to one, since the label of  $\mathbf{x}_i$  is unknown.

A remarkable strength of the proposed model is the further extension to deal with the challenge of OSDA. In order to detect the unknown classes in the target domain, we reformulate the matrix  $\mathbf{Y}$  as  $\tilde{\mathbf{Y}} = [\tilde{\mathbf{Y}}_1, \dots, \tilde{\mathbf{Y}}_n] \in \mathbf{R}^{n \times (C+1)}$ . For the labeled data,  $\tilde{\mathbf{Y}}_{ij} = 1$  if  $\mathbf{x}_i$  is labeled as  $j$  and  $\tilde{\mathbf{Y}}_{ij} = 0$  otherwise. For the unlabeled data  $\mathbf{x}_i$ ,  $\tilde{\mathbf{Y}}_{ij} = 1$  if  $j = C+1$  and  $\tilde{\mathbf{Y}}_{ij} = 0$  otherwise. Then we obtain the soft labels  $\tilde{\mathbf{F}} \in \mathbf{R}^{n \times (C+1)}$ , where the last column of matrix  $\tilde{\mathbf{F}}$  represents the probabilities that the data samples belong to the unknown classes. Similarly, we set  $\alpha_i$  as zero in the source domain to enable their resulted labels unchanged. However,  $\alpha_i$  should be set as a positive value between one and zero, the smaller  $\alpha_i$  is, and the easier one sample is to be classified as unknown classes. The extreme case is  $\alpha_i = 1$  which means that the resulted label of  $\mathbf{x}_i$  will definitely be 1 to  $C$ , and thus lose the capability to discover the unknown classes. Another extreme case is  $\alpha_i = 0$  which means that the resulted label of  $\mathbf{x}_i$  will definitely be classified as unknown class, and thus lose the identify ability.

Once we obtain the new soft labels  $\tilde{\mathbf{F}}$ , the class scatter matrix could be computed by Eq. (2) and Eq. (3) using  $\tilde{\mathbf{F}}_{com} = \tilde{\mathbf{F}}(:, 1 : C)$ . As for the class-wise MMD matrix, we assume that  $\mathbf{A} = \mathbf{B}$  for simplicity, and it is computed as follows:

$$\begin{aligned} & \sum_{i=1}^C \left\| \frac{1}{n_s^{(i)}} \sum_{j=1}^{n_s} \tilde{\mathbf{F}}_{ji} \mathbf{A}^T \mathbf{x}_j - \frac{1}{n_t^{(i)}} \sum_{j=n_s+1}^{n_s+n_t} \tilde{\mathbf{F}}_{ji} \mathbf{A}^T \mathbf{x}_j \right\|^2 \\ &= \sum_{i=1}^C \text{tr}(\mathbf{A}^T \tilde{\mathbf{M}}^{(i)} \mathbf{A}), \end{aligned} \quad (19)$$

where  $\tilde{\mathbf{M}}^{(i)} = \tilde{\mathbf{X}} \tilde{\mathbf{L}}^{(i)} \tilde{\mathbf{X}}^T$ ,  $\tilde{\mathbf{L}}^{(i)} = \sum_{j=1}^C \tilde{\mathbf{F}}^{(i)} \bullet \tilde{\mathbf{e}}^{(i)} \bullet \tilde{\mathbf{e}}^{(i)T} \bullet \tilde{\mathbf{F}}^{(i)}$ ,  $\tilde{\mathbf{F}}^{(i)} = \text{diag}(\tilde{\mathbf{F}}(:, i))$ ,  $\tilde{\mathbf{e}}^{(i)}(1 : n_s) = 1 / \sum_{j=1}^{n_s} \tilde{\mathbf{F}}(j, i)$ ,  $\tilde{\mathbf{e}}^{(i)}(n_s + 1 : n) = -1 / \sum_{j=n_s+1}^n \tilde{\mathbf{F}}(j, i)$ ,  $\tilde{\mathbf{e}}^{(i)} \in \mathbf{R}^{n \times 1}$ . As for the MMD matrix, we divide the samples into two classes, i.e., the shared class and private class. Then the soft labels could be defined as  $\hat{\mathbf{F}} = [\hat{\mathbf{f}}_1, \hat{\mathbf{f}}_2] \in \mathbf{R}^{n \times 2}$ , where  $\hat{\mathbf{f}}_1 = \sum_{i=1}^C \tilde{\mathbf{F}}(:, i)$ , and  $\hat{\mathbf{f}}_2 = \tilde{\mathbf{F}}(:, C+1)$ . Now the MMD can be reformulated by  $\hat{\mathbf{F}}$  as the class-wise MMD did, while we only adopt the first shared class MMD matrix since there are no private class in the source domain, i.e.,  $\hat{\mathbf{M}}^{(1)}$ . It is obvious that the vector  $\hat{\mathbf{f}}_1$  means that the probability of each sample belonging to the common class, which alleviate the negative transfer incurred by the unknown classes in a weighted mechanism. Finally, the proposed model Eq. (19) could be easily extended to the OSDA scenario using this modified GLP approach, while we assume that  $\mathbf{A} = \mathbf{B}$  for simplicity. The final OSDA model is as follows:

$$\begin{aligned} & \max_{\mathbf{A}} \text{tr}(\mathbf{A}^T \mathbf{S}_t \mathbf{A}) - \text{tr}(\mathbf{F}^T \mathbf{L} \mathbf{F}) - \text{tr}((\mathbf{F} - \mathbf{Y})^T \mathbf{U} \mathbf{H} (\mathbf{F} - \mathbf{Y})) \\ & \text{s.t.} \quad \text{tr}(\mathbf{A}^T \hat{\mathbf{M}}^{(1)} \mathbf{A}) + \sum_{i=1}^C \text{tr}(\mathbf{A}^T \tilde{\mathbf{M}}^{(i)} \mathbf{A}) \\ & \quad + \gamma_{st} \text{tr}(\mathbf{A}^T \mathbf{S}_w \mathbf{A}) + \gamma \|\mathbf{A}\|_F^2 = 1. \end{aligned} \quad (20)$$

### C. Optimization and Algorithm

In this section, we only discuss the optimization and algorithm about the CSDA model (18), while similar procedures on the OSDA are not shown due to space limitation. Unfortunately, it is difficult to jointly optimize  $\mathbf{Q}$  and  $\mathbf{F}$ , thus we follow the previous work [11] and it is solvable over each of them in a leave-one-out manner. Specifically, we explore an EM-like optimization scheme to update the variables. For **E**-step, we fix  $\mathbf{Q}$  and update  $\mathbf{F}$ , while for **M**-step, we update subspace projection  $\mathbf{Q}$  using the updated  $\mathbf{F}$ . Hence, we optimize two sub-problems iteratively.

1) **E-step: Label Propagation:** We utilize the transferred features during the current iteration to compute  $\mathbf{L}$ , thus we obtain the partial derivative of Eq. (18) w.r.t.,  $\mathbf{F}$ , by setting it to zero as:

$$\mathbf{L} \mathbf{F} + \mathbf{U} \mathbf{H} (\mathbf{F} - \mathbf{Y}) = \mathbf{0} \quad (21)$$

Note that  $\mathbf{P} = \mathbf{H}^{-1} \mathbf{W}$ , then the solution can be derived as follows:

$$\begin{aligned} \mathbf{F}^* &= (\mathbf{L} + \mathbf{U} \mathbf{H})^{-1} \mathbf{U} \mathbf{H} \mathbf{Y} = (\mathbf{I} - \mathbf{P} + \mathbf{U})^{-1} \mathbf{U} \mathbf{Y} \\ &= (\mathbf{I}_\alpha - \mathbf{I}_\alpha \mathbf{P} + \mathbf{I}_\beta)^{-1} \mathbf{I}_\beta \mathbf{Y} = (\mathbf{I} - \mathbf{I}_\alpha \mathbf{P}) \mathbf{I}_\beta \mathbf{Y}, \end{aligned} \quad (22)$$

where  $\mathbf{I} \in \mathbf{R}^{n \times n}$  is an identify matrix,  $\mathbf{I}_\alpha \in \mathbf{R}^{n \times n}$  is a diagonal matrix with the  $i$ -th entry being  $\alpha_i$ , and  $\mathbf{I}_\beta = \mathbf{I} - \mathbf{I}_\alpha$ .

2) **M-step: Learning Subspace Projection:** When  $\mathbf{F}$  is optimized, we could update the subspace projection  $\mathbf{Q}$  with the refined class-wise MMD and class scatter matrix. According to the constrained optimization theory, we denote  $\Phi = \text{diag}(\phi_1, \dots, \phi_k) \in \mathbf{R}^{k \times k}$  as the Lagrange multiplier, and derive the Lagrange function for Eq. (19) w.r.t.,  $\mathbf{Q}$  as follows:

$$\begin{aligned} L_g &= \text{tr}(\mathbf{Q}^T \begin{bmatrix} \mathbf{S}_t^{(s)} & \mathbf{0} \\ \mathbf{0} & \tilde{\mathbf{S}}_t^{(t)} \end{bmatrix} \mathbf{Q}) \\ &+ \text{tr}(((\sum_{i=0}^C \mathbf{Q}^T \begin{bmatrix} \mathbf{S} \mathbf{T}_1^{(i)} & \mathbf{S} \mathbf{T}_2^{(i)} \\ \mathbf{S} \mathbf{T}_3^{(i)} & \mathbf{S} \mathbf{T}_4^{(i)} \end{bmatrix} \mathbf{Q}) - \mathbf{I}_{2m}) \Phi), \end{aligned} \quad (23)$$

then setting it to zeros as follows:

$$\begin{bmatrix} \mathbf{S}_t^{(s)} & \mathbf{0} \\ \mathbf{0} & \mathbf{S}_t^{(t)} \end{bmatrix} \mathbf{Q} = \sum_{i=1}^C \left( \begin{bmatrix} \mathbf{S} \mathbf{T}_1^{(i)} & \mathbf{S} \mathbf{T}_2^{(i)} \\ \mathbf{S} \mathbf{T}_3^{(i)} & \mathbf{S} \mathbf{T}_4^{(i)} \end{bmatrix} \right) \mathbf{Q} \Phi \quad (24)$$

Finally, finding the optimal adaptation matrix  $\mathbf{Q}$  is reduced to solve Eq. (24) for the  $k$  leading eigenvalues, and the corresponding eigenvectors, which can be solved analytically through generalized eigenvalue decomposition. Once the transformation matrix  $\mathbf{Q}$  is obtained, the projections  $\mathbf{A}$  and  $\mathbf{B}$  can be obtained easily.

What is noteworthy is that, by alternating the **E** and **M** steps detailed above, we will iteratively optimize the problem until the objective function becomes converged, and we are able to alternatively enhance the quality of predicted labels and transferred features. A complete procedure of PFSLG-DA for CSDA is summarized in Algorithm 1.

**Algorithm 1: PFSLG-DA for CSDA**


---

**Input:** source and target domain data  $X$ , source domain labels  $Y_s$ , subspace bases  $k$ , parameters  $\delta, \lambda, \gamma, \gamma_{st}$ , iterations  $T$

**Output:** target domain labels  $Y_t$

**Begin**

**Initialization**

1. Compute  $S_t^{(s)} = X_s X_s^T, S_t^{(t)} = X_t X_t^T, S_w^{(s)}$  by Eq. (3),  $M_s^{(0)}, M_t^{(0)}, M_{st}^{(0)}, M_{ts}^{(0)}$  by Eq. (5)-(8)
2. Predict  $F$  by GLP using original features
3. Compute  $S_w^{(t)}, M_s^{(i)}, M_t^{(i)}, M_{st}^{(i)}, M_{ts}^{(i)}$  ( $i = 1, \dots, C$ ) by Eq. (10)-(13)
4. Update the transferred features  $Z_s$  and  $Z_t$  by Eq. (24), and  $Z_s = A^T X_s, Z_t = B^T X_t$

**Repeat until convergence**

5. Construct the graph  $L$  on  $Z = [Z_s, Z_t]$ , obtain the soft labels  $F$  by Eq. (22) and the hard labels by  $y_i = \arg\max_c F_{ic} (1 \leq i \leq n)$
6. Model the soft labels-based class-wise MMD and class scatter matrix  $S_w^{(t)}, M_s^{(i)}, M_t^{(i)}, M_{st}^{(i)}, M_{ts}^{(i)}$  by Eq. (3) and Eq. (5)-(8)
7. Update the transferred features  $Z_s$  and  $Z_t$  by Eq. (24), and  $Z_s = A^T X_s, Z_t = B^T X_t$

**End repeat**

**Return** target domain labels  $Y_t$  formed by  $y_i (1 \leq i \leq n_t)$

---

**D. Computational Complexity**

Now we analyze the computational complexity of Algorithm 1 by the big  $O$  notation. As stated above,  $X_s \in \mathbf{R}^{m \times n_s}, X_t \in \mathbf{R}^{m \times n_t}, X = [X_s, X_t] \in \mathbf{R}^{m \times n}, A, B \in \mathbf{R}^{m \times k}$ , where  $m$  is the original dimensionality,  $k$  is the dimensionality of the subspace,  $n = n_s + n_t$  is the number of all samples. We denote the number of classes as  $C$  and the number of iterations as  $T$ . The time cost of Algorithm 1 consists of the following two parts:

- 1) Computing the soft labels-based class-wise MMD and class scatter matrix in step 6 costs  $O(Tmn_t^2 + Tm^2n_t + TCn_t^2 + TC^2n_t)$  and  $O(TCn_s^3 + TCn_t^3 + TCn_sn_t^2 + TCn_s^2n_t)$ .
- 2) Solving the eigendecomposition problem in step 7 costs  $O(Tmk^2)$ .

Then, the overall computational complexity of Algorithm 1 is  $O(Tmn_t^2 + Tm^2n_t + TCn_t^2 + TC^2n_t + TCn_s^3 + TCn_t^3 + TCn_sn_t^2 + TCn_s^2n_t + TCn_s^3 + TCn_t^3 + TCn_sn_t^2 + TCn_s^2n_t)$ . In section IV, we will show that the number of iterations  $T$  is usually smaller than 10, which is enough to guarantee convergence. Besides, the typical values of  $k$  are not greater than 200, so  $T \ll \min(m, n), k \ll \min(m, n)$ . Therefore, Algorithm 1 can be solved in polynomial time with respect to the number of samples.

**IV. EXPERIMENTS****A. Datasets Description**

We adopted 5 benchmark datasets in cross-domain object recognition to validate the effectiveness of the proposed approach, namely USPS+MNIST, COIL20, MSRC+VOC2007,

Office31+Caltech256, Office-Home. The dataset descriptions are introduced as follows:

**USPS+MNIST:** From Fig. 1, we see that USPS and MNIST follow very different distributions. Specifically, USPS dataset consists of 9,298 images of size  $16 \times 16$ , while MNIST dataset has 70,000 examples of size  $28 \times 28$ . They share 10 semantic classes, each corresponding to one digit. For a fair comparison, we adopt their subsets constructed by most previous work [6], [7], [34], where 1,800 images are randomly sampled in USPS and 2,000 images in MNIST. For convenience, we denote the datasets USPS, MNIST by U and M, then 2 DA tasks can be constructed, namely  $U \rightarrow M, M \rightarrow U$ . Note that the arrow " $\rightarrow$ " is the direction from source to target. For example,  $U \rightarrow M$  means USPS is the labeled source domain while MNIST is the unlabeled target domain.

**COIL20:** COIL20 is sampled from 20 objects and consists of 1,440 images of size  $32 \times 32$ , where each object rotates 5 degrees successively and derives 72 images. Moreover, COIL20 could be divided into COIL1 and COIL2, and their distributions are different, because COIL1 locates in  $[0^\circ, 85^\circ, ] \cup [180^\circ, 265^\circ]$  while COIL2 locates in  $[90^\circ, 175^\circ, ] \cup [270^\circ, 355^\circ]$ . Likewise, 2 DA tasks can be constructed, namely  $C1 \rightarrow C2, C2 \rightarrow C1$ .

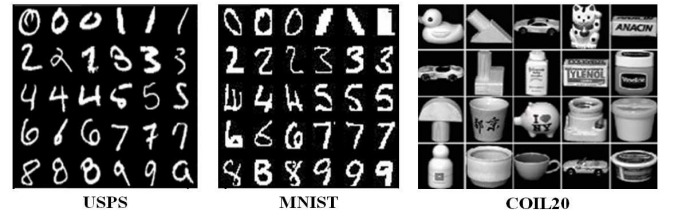


Fig. 1: Exemplary images from USPS+MNIST and COIL20

**MSRC+VOC2007:** From Fig. 2, we see that they follow different distributions, since MSRC is from standard images for evaluations, while VOC2007 is from digital photos in Flickr7. MSRC has more than 4,000 samples from 18 categories, while VOC2007 includes over 5,000 samples annotated with 20 concepts. Similarly, we follow previous work [34], [50] and select 6 shared semantic classes (1,269 images in MSRC and 1,530 images in VOC2007). Furthermore, Dense SIFT features are used with 128 dimensions, then 2 DA tasks can be constructed, namely  $Ms \rightarrow Vo, Vo \rightarrow Ms$ .

**Office31+Caltech256:** Office-31 dataset consists of three domains, namely Amazon, Webcam and DSLR, and contains 4,652 images from 31 categories. Caltech256 dataset has over 30,000 samples from 256 categories. Fig. 3 illustrates some sample images from each domain, and they follow very different distributions. As for CSDA, we follow previous work [6], [7] and select 10 shared categories from each domain, where the SURF features with 800 dimensions are adopted. In order to further evaluate our approach in OSDA, we adopt Office-31 dataset and follow previous OSDA work [15], [16] using the same set of known shared classes, and the same unknown private classes in the target domain. For a fair comparison, the deep features are adopted, which is pre-extracted from the AlexNet model [51] (Fc7) and the ResNet-50 [52] model pretrained on ImageNet. Moreover, we denote





Fig. 2: Exemplary images from MSRC+VOC2007



Fig. 3: Exemplary images from Office31+Caltech256

the dataset Amazon, Webcam, Dslr, and Caltech by A, W, D, and C. Then  $4 \times 3 = 12$  DA tasks can be constructed in CSDA, while  $3 \times 2 = 6$  DA tasks in OSDA.

**Office-Home:** It was released recently as a more challenging DA dataset [53], crawled through several search engines and online image directories. As shown in Fig. 4, it consists of 4 different domains: Artistic images (Ar), Clipart images (Cl), Product images (Pr) and Real-World images (Rw). In total, there are 65 object categories for each domain and 15,500 images in the whole dataset. As for CSDA, we use the images from all 65 categories, and  $4 \times 3 = 12$  DA tasks can be constructed. As for OSDA, we follow the previous work [7], [8], and choose (in alphabetic order) the first 25 classes shared by the source and target domains, while the 26-65 classes belong to the unknown classes in the target domain. We also construct OSDA tasks between each two domains in both directions and form 12 tasks. For a fair comparison, we utilize the deep features pre-extracted from the ResNet-50 [52] model pre-trained on ImageNet.

### B. Protocols

Our approach could not only handle CSDA difficulties but also OSDA. In this section, we first report the CSDA results. Then, we report the results of OSDA. For the process of data pre-treatment, we normalize all of the data and then z-score them to have zero mean and unit standard deviation in each dimension. For the parameters, we fix the number of iterations  $T = 5$ , and 20-nearest neighbor graph is adopted with Euclidean distance-based weight for simplicity. For different experimental datasets, we set different values for the hyper-parameters to gain good performance. Specifically, when evaluating our approach on USPS+MNIST, we set  $k = 100$ ,  $\lambda = 1$ ,  $\gamma = 0.1$ ,  $\gamma_{st} = 0.01$ ,  $\delta = 1$ . For COIL20, we set  $k = 20$ ,  $\lambda = 1$ ,  $\gamma = 0.01$ ,  $\gamma_{st} = 0.01$ ,  $\delta = 1$ . For MSRC+VOC2007, we set  $k = 20$ ,  $\lambda = 0.5$ ,  $\gamma = 0.05$ ,  $\gamma_{st} = 0.01$ ,  $\delta = 0$ . For Office31+Caltech256, we set  $k = 20$ ,  $\lambda = 0.5$ ,  $\gamma = 0.05$ ,  $\gamma_{st} = 0.01$ ,  $\delta = 0.1$ . For Office-Home, we set  $k = 100$ ,

$\lambda = 1$ ,  $\gamma = 0.5$ ,  $\gamma_{st} = 0.1$ ,  $\delta = 1$ . As for OSDA scenario, we set  $k = 100$ ,  $\gamma = 1$ ,  $\gamma_{st} = 0.1$  on all datasets. Although there are so many parameters that has to tune, all of them have interpretable physical meanings and can achieve optimal performance under a wide range. Moreover, in this paper, since we just focus on the challenging unsupervised DA and there are no labeled target samples, we follow previous work [7], [42], and set the hyper-parameters by searching a wide range and use the optimal ones. In semi-supervised domain adaptation, one can deploy cross-validation to tune them.

It is noteworthy that this paper proposes a mechanism to filter out the small probabilities in soft labels in case they influence the final performance, where we only select several top values from each soft label sorted in a descending order. Moreover, in CSDA, we set  $\alpha_i = 0$  for the labeled data and  $\alpha_i = 1$  for the unlabeled data, because there are no unknown classes in the target domain. As for OSDA, we also set  $\alpha_i = 0$  for the labeled data, while  $\alpha_i$  for the unlabeled data should be set to a positive value between 0 and 1, so as to detect those unknown classes in the target domain and match the common classes between domains correctly.

We follow the the experimental protocols in [5], [6] to perform CSDA, and the datasets of USPS+MNIST, COIL20, MSRC+VOC2007, Office31+Caltech256, Office-Home are tested. Several state-of-the art approaches are tested for comparison, *e.g.*, Transfer Component Analysis (TCA) [8], Transfer Joint Matching (TJM) [32], Joint Distribution Adaptation (JDA) [7], Balanced Distribution Adaptation (BDA) [33], Visual Domain Adaptation (VDA) [9], Scatter Component Analysis (SCA) [10], Domain Invariant and Class Discriminative (DICD) [5], Discriminative Label Consistent (DLC) [45], Geodesic Flow Kernel (GFK) [42], Subspace Alignment (SA) [47], Subspace Distribution Alignment (SDA) [48], Probabilistic Unsupervised Domain Adaptation (PUnDA) [29], Joint Geometrical and Statistical Alignment (JGSA) [6], ResNet-50 [52], Deep Adaptation Network (DAN) [30], Domain-Adversarial training of Neural Networks (DANN) [54], Joint Adaptation Networks (JAN) [31], Conditional Adversarial Domain Adaptation (CDAN-RM, CDAN-M) [55].

For OSDA, we follow the same settings in previous work [13], [15], [16], and the datasets of Office-Home and Office-31 are tested. Since the OSDA research is rarely reported, we compare our approach with not only the latest OSDA methods, *i.e.*, Assign-and-Transform-Iteratively (ATI- $\lambda$ ) [13], Open Set Back-Propagation (OSBP) [15], OpenMax [56], Separate to Adapt (STA) [16], but also some non-OSDA methods, *i.e.*, ResNet-50 [52], DANN [54], DAN [30], Residual Transfer Networks (RTN) [57], (Unsupervised Domain Adaptation by Backpropagation) UDABP [23].

### C. Results and Discussions

Comparing with the shallow FDA methods, the results of CSDA on USPS+MNIST, COIL20, MSRC+VOC2007, Office31+Caltech256 are shown in Table. I, II, III, IV. It can be seen that our approach outperforms state-of-the-art methods on all of the 18 evaluations. The average classification accuracies on different datasets of our method are 79.56%, 99.72%,





Fig. 4: Exemplary images from Office-Home

TABLE I: Accuracy (%) on the USPS+MNIST dataset (CSDA)

Task	TCA	TJM	JDA	BDA	VDA	SCA	DICD	GFK	SA	SDA	JGSA	Our
U→M	51.20	52.25	59.65	59.35	62.95	48.00	65.20	46.45	48.80	35.70	68.15	<b>73.40</b>
M→U	56.33	63.28	67.28	69.78	74.72	65.11	77.83	61.22	67.78	65.00	80.44	<b>85.72</b>
Avg.	53.77	57.77	63.47	64.57	68.84	56.56	71.52	53.84	58.29	50.35	74.30	<b>79.56</b>

TABLE II: Accuracy (%) on the COIL20 dataset (CSDA)

Task	TCA	TJM	JDA	BDA	VDA	DICD	GFK	JGSA	Our
C1→C2	88.47	91.67	89.31	97.22	99.31	95.69	72.50	91.25	<b>100.0</b>
C2→C1	85.83	91.53	88.47	96.81	97.92	93.33	74.17	91.25	<b>99.44</b>
Avg.	87.15	91.60	88.89	97.02	98.62	94.51	73.34	91.25	<b>99.72</b>

TABLE III: Accuracy (%) on the MSRC+VOC2007 dataset (CSDA)

Task	TCA	TJM	JDA	SCA	GFK	SA	JGSA	Our
Ms→Vo	31.70	32.48	30.72	32.75	30.63	30.90	33.20	<b>40.13</b>
Vo→Ms	45.78	46.34	43.50	48.94	44.47	46.88	48.86	<b>63.91</b>
Avg.	38.74	39.41	37.11	40.85	37.55	38.89	41.03	<b>52.02</b>

52.02%, 58.04%, which have 5.26%, 1.10%, 10.99%, 7.26% improvements compared with the best baselines JGSA, VDA, JGSA, DLC, respectively.

TCA, TJM, JDA and BDA aimed to exploit shared features with inter-domain distributional alignment, while VDA, SCA, DICD, DLC further considered the intra-domain data properties. They usually assumed that there exists a common space where those issues could be optimized simultaneously, while it will fail when the two different domains have large discrepancy. On the contrary, GFK, SA and SDA exploited the domain-specific features by manipulating the subspaces of the two domains such that the subspace of each individual domain all contributes to the final mapping. However, the distributional shift between projected data of two domains is ignored. Therefore, PUnDA and JGSA were proposed to jointly reduce the inter-domain distributional differences and preserve the intra-domain data properties with two coupled projections. However, all of them reformulates the class-wise statistics (e.g., class-wise MMD and class scatter matrices) using the hard labels that might result in negative transfer. For instance, the performance of DICD is worse than VDA on tasks like  $C \rightarrow D$ ,  $A \rightarrow W$ ,  $A \rightarrow D$ ,  $D \rightarrow A$ , although DICD constructed the hard labels-based class scatter matrices to preserve the discriminative information of target domain while VDA did not. Furthermore, the same problem happens to

JGSA and its performance is even worse than PUnDA on tasks like  $W \rightarrow C$ ,  $W \rightarrow A$ ,  $D \rightarrow C$ ,  $D \rightarrow A$ , where JGSA utilized the hard labels-based class-wise MMD but PUnDA did not. Based on these observations, we speculate that the behavior of hard labels-based class-wise statistics mainly depends on the quality of hard labels, and the number of target samples compared to the source domain. Different from them, we reformulate them using the filtered soft labels, thus the proposed approach could achieve best results among them.

The results of CSDA on Office-Home dataset with ResNet-50 features are shown in Table. V. To verify the effectiveness of the proposed method, we also report the results of six end-to-end deep models, i.e., ResNet-50, DAN, DANN, JAN, CDAN-RM and CDAN-M. From the results in Table. V, we can see that our approach also outperforms the deep FDA models. Specifically, our approach achieves 3.4% improvement against the best baseline CDAN-M. Compared with shallow FDA methods, deep FDA methods integrate feature extraction and knowledge transfer into a shared network and achieve promising results. However, some techniques, which has been proven effective in domain adaptation, are hard to be implemented with deep structure. For example, the class-wise MMD can be easily optimized by matrix operations but it is very tricky in deep networks [5]. In addition, the results on Office-Home verify that our method is applicable to large-scale

TABLE IV: Accuracy (%) on the Office31+Caltech256 dataset (CSDA)

Task	TCA	TJM	JDA	BDA	VDA	SCA	DICD	DLC	GFK	SA	SDA	PUnDA	JGSA	Our
C→A	45.82	46.76	45.62	44.89	46.14	43.74	47.29	54.18	46.03	49.27	49.69	50.10	51.46	<b>61.38</b>
C→W	31.19	38.98	41.69	38.64	46.10	33.56	46.44	52.59	36.95	40.00	38.98	41.70	45.42	<b>61.36</b>
C→D	34.39	44.59	45.22	47.77	51.59	39.49	49.68	47.77	40.76	39.49	40.13	45.80	45.86	<b>57.96</b>
A→C	42.39	39.45	39.36	40.78	42.21	38.29	42.39	43.72	40.69	39.98	39.54	39.50	41.50	<b>47.64</b>
A→W	36.27	42.03	37.97	39.32	51.19	33.90	45.08	43.39	36.95	33.22	30.85	42.50	45.76	<b>55.59</b>
A→D	33.76	45.22	39.49	43.31	48.41	34.21	38.85	42.68	40.13	33.76	33.76	40.30	47.13	<b>52.23</b>
W→C	29.39	30.19	31.17	28.94	27.60	30.63	33.57	38.29	24.76	35.17	34.73	36.50	33.21	<b>41.23</b>
W→A	28.91	29.96	32.78	32.99	26.10	30.48	34.13	39.87	27.56	39.25	39.25	42.40	39.87	<b>45.41</b>
W→D	89.17	89.17	89.17	91.72	89.18	92.36	89.81	85.99	85.35	75.16	75.80	85.20	90.45	<b>94.90</b>
D→C	30.72	31.43	31.52	32.50	31.26	32.32	34.64	32.41	29.30	34.55	35.89	38.90	29.92	<b>37.93</b>
D→A	31.00	32.78	33.09	33.09	37.68	33.72	34.45	38.20	28.71	39.87	38.73	40.30	38.00	<b>47.29</b>
D→W	86.10	85.42	89.49	91.86	90.85	88.81	91.19	90.22	80.34	76.95	76.95	83.20	91.86	<b>93.56</b>
Avg.	43.26	46.33	46.38	47.15	49.03	44.29	48.96	50.78	43.13	44.72	44.53	48.86	50.04	<b>58.04</b>

TABLE V: Accuracy (%) on the Office-Home dataset (CSDA)

Task	ResNet-50	DAN	DANN	JAN	CDAN-RM	CDAN-M	Our
Ar→Cl	34.9	43.6	45.6	45.9	49.6	50.7	<b>58.8</b>
Ar→Pr	50.0	57.0	59.3	61.2	70.8	70.6	<b>77.3</b>
Ar→Rw	58.0	67.9	70.1	68.9	75.4	76.0	<b>79.3</b>
Cl→Ar	37.4	45.8	47.0	50.4	57.1	57.6	<b>60.9</b>
Cl→Pr	41.9	56.5	58.5	59.7	70.6	70.0	<b>76.1</b>
Cl→Rw	46.2	60.4	60.9	61.0	70.1	70.0	<b>73.2</b>
Pr→Ar	38.5	44.0	46.1	45.8	58.0	57.4	<b>61.4</b>
Pr→Cl	31.2	43.6	43.7	43.4	47.6	50.9	<b>53.3</b>
Pr→Rw	60.4	67.7	68.5	70.3	76.2	77.3	<b>79.3</b>
Rw→Ar	53.9	63.1	63.2	63.9	69.2	70.9	69.6
Rw→Cl	41.2	51.5	51.8	52.4	55.8	56.7	<b>58.5</b>
Rw→Pr	59.9	74.3	76.8	76.8	81.6	81.6	<b>83.0</b>
Avg.	46.1	56.3	57.6	58.3	65.2	65.8	<b>69.2</b>

TABLE VI: Accuracy (%) on the Office-Home dataset (OSDA, OS)

Task	ResNet-50	DANN	ATI-λ	OSBP	OpenMax	STA	Our
Ar→Cl	53.4	54.6	55.2	56.7	56.5	58.1	<b>61.9</b>
Ar→Pr	69.3	69.5	69.1	67.5	69.1	71.6	<b>74.3</b>
Ar→Rw	78.7	80.2	79.2	80.6	80.3	85.0	<b>87.6</b>
Cl→Ar	61.4	61.9	61.7	62.5	64.1	63.4	<b>66.5</b>
Cl→Pr	61.8	63.5	63.5	65.5	64.8	<b>69.3</b>	<b>69.3</b>
Cl→Rw	71.0	71.7	72.9	74.7	73.0	75.8	<b>79.0</b>
Pr→Ar	64.0	63.3	64.5	64.8	64.0	65.2	<b>69.7</b>
Pr→Cl	52.7	49.7	52.6	51.5	52.9	53.1	<b>54.3</b>
Pr→Rw	74.9	74.2	75.8	71.5	76.9	80.8	<b>83.9</b>
Rw→Ar	70.0	71.3	70.7	69.3	71.2	74.9	<b>77.8</b>
Rw→Cl	51.9	51.9	53.5	49.2	53.7	54.4	<b>58.6</b>
Rw→Pr	74.1	72.9	74.1	74.0	74.5	81.9	<b>85.9</b>
Avg.	65.3	65.4	66.1	65.7	66.7	69.5	<b>72.4</b>

dataset and is able to achieve favorable accuracy. Furthermore, our method generally runs faster than deep ones since we use off-the-shelf features.

For OSDA problem, we evaluate our model on Office-Home dataset with ResNet-50 features, Office31 dataset with Fc7 features and ResNet-50 features, and their results are reported in Table. VI, VII, VIII. Following previous work [15], [16], we employ 3 evaluation metrics: OS: normalized accuracy for all classes including the unknown as one class; OS\*: normalized accuracy only on known classes; UNK: the accuracy of unknown samples. In compared experiments, we study the OS accuracy on Office-Home dataset, while OS, OS\* and UNK accuracies are evaluated on Office31 dataset. Different from them, this paper tests all thoes three metrics

on Office-Home dataset in the model analysis section, since our target is to not only realize the correct knoledge transfer, but also the unknown classes detection. From the compared results, it is clear that the DA algorithms perform better than non-DA method of ResNet-50. Furthermore, the approaches for OSDA problem work better than CSDA-based method DANN, DAN RNT and UDABP, because the unknown classes in the target domain might bring negative transfer. Among the OSDA-based methods, the average OS accuracy of our method on Office-Home are 72.4%, which has 2.9% improvement compared with the best baseline STA. The average OS, OS\*, UNK accuracies on Office31 dataset with Fc7 features and ResNet-50 features are 86.4%, 86.3%, 87.0% and 95.5%, 96.3%, 87.3%, respectively. The results further verify that our

TABLE VII: Accuracy (%) on the Office31 dataset (OSDA, OS, OS\*, UNK)

Task(Fc7)	Metric	DAN	RTN	UDABP	ATI- $\lambda$	Our
A→D	OS	77.6	76.6	78.3	79.8	<b>80.4</b>
	OS*	76.5	74.7	77.3	79.2	<b>79.9</b>
	UNK	-	-	-	85.8	<b>86.0</b>
A→W	OS	72.5	73.0	75.9	77.6	<b>79.5</b>
	OS*	70.2	70.8	73.8	76.5	<b>78.6</b>
	UNK	-	-	-	88.6	<b>88.8</b>
D→A	OS	57.0	57.2	57.6	71.3	<b>76.6</b>
	OS*	53.5	53.8	54.1	70.0	<b>75.6</b>
	UNK	-	-	-	84.3	<b>87.0</b>
D→W	OS	88.4	89.0	89.8	93.5	<b>96.8</b>
	OS*	87.5	88.1	88.9	93.2	<b>97.3</b>
	UNK	-	-	-	<b>96.5</b>	91.6
W→A	OS	60.8	62.4	64.0	76.7	<b>86.3</b>
	OS*	58.5	60.2	61.8	76.5	<b>86.9</b>
	UNK	-	-	-	78.7	<b>81.0</b>
W→D	OS	98.3	98.8	98.7	98.3	<b>98.5</b>
	OS*	97.5	98.3	98.0	99.2	<b>99.6</b>
	UNK	-	-	-	<b>89.3</b>	87.6
Avg.	OS	75.8	76.2	77.4	82.9	<b>86.4</b>
	OS*	74.0	74.3	75.7	82.4	<b>86.3</b>
	UNK	-	-	-	<b>87.2</b>	87.0

TABLE VIII: Accuracy (%) on the Office31 dataset ((OSDA, OS, OS\*, UNK))

Task(ResNet-50)	Metric	ResNet-50	RTN	DANN	ATI- $\lambda$	OSBP	STA	Our
A→D	OS	85.2	89.5	86.5	84.3	88.6	93.7	<b>94.9</b>
	OS*	85.5	90.1	87.7	86.6	89.2	96.1	<b>96.5</b>
	UNK	-	-	-	61.3	<b>82.6</b>	69.7	78.7
A→W	OS	82.5	85.6	85.3	87.4	86.5	89.5	<b>92.1</b>
	OS*	82.7	88.1	87.7	88.9	87.6	92.1	<b>92.7</b>
	UNK	-	-	-	72.4	75.5	63.5	<b>85.7</b>
D→A	OS	71.6	72.3	75.7	78.0	88.9	89.1	<b>96.0</b>
	OS*	71.5	72.8	76.2	79.6	90.6	93.5	<b>96.6</b>
	UNK	-	-	-	62.0	71.9	45.1	<b>90.4</b>
D→W	OS	94.1	94.8	97.5	93.6	97.0	97.5	<b>98.3</b>
	OS*	94.3	96.2	98.3	95.3	96.5	96.5	<b>99.3</b>
	UNK	-	-	-	76.6	<b>100.0</b>	<b>100.0</b>	88.1
W→A	OS	75.5	73.5	74.9	80.4	85.8	87.9	<b>92.7</b>
	OS*	75.2	73.9	75.6	81.4	84.9	87.4	<b>92.7</b>
	UNK	-	-	-	70.4	<b>94.8</b>	92.9	93.5
W→D	OS	96.6	97.1	<b>99.5</b>	96.5	97.9	<b>99.5</b>	98.9
	OS*	97.0	98.7	<b>100.0</b>	98.7	98.7	99.6	<b>100.0</b>
	UNK	-	-	-	74.5	89.9	<b>98.5</b>	87.6
Avg.	OS	84.3	85.5	86.6	86.7	90.8	92.9	<b>95.5</b>
	OS*	84.4	86.6	87.6	88.4	91.3	94.2	<b>96.3</b>
	UNK	-	-	-	69.5	85.8	78.3	<b>87.3</b>

approach not only mitigate the distributional shift between domains greatly, but also detect the unknown classes in the target domain correctly.

#### D. Model Analysis

In this section, we analyze our approach by discussing the effectiveness of the probabilistic soft labels guided class-wise statistics (*i.e.*, class-wise MMD and class scatter matrice), the filtering mechanism in soft labels, the relationships between the inter-domain distributional alignment and the intra-domain discriminative preservation, the essential capability to annotate

the common and unknown classes in OSDA, the parameter sensitivity.

Fig. 5 and Fig. 6 illustrate the results on datasets of Office31+Caltech256 and Office-Home, where the class-wise statistics here are formulated using the hard labels, the original soft labels, and the filtered soft labels, respectively. By comparing the results with hard labels and results with original soft labels, we can easily capture that the approach with original soft labels behaves badly on the most tasks, which proves that the model stability might be influenced by the small probabilities in original soft labels. It is noteworthy that the

TABLE IX: Accuracy (%) on different datasets with varying numbers of selected maximal probabilities (CSDA)

Number	1	2	3	4	5	6	7	8	9	All
USPS+MNIST	78.87	79.29	<b>79.51</b>	79.41	79.41	79.31	79.31	79.33	79.48	79.17
COIL20	<b>99.66</b>	99.65	99.45	99.10	99.03	99.17	99.24	99.24	99.24	98.54
MSRC+VOC2007	50.79	51.59	<b>51.92</b>	51.69	51.66	-	-	-	-	50.05
Office31+Caltech256	55.81	57.15	57.33	57.41	57.55	<b>57.56</b>	57.51	57.50	57.25	55.79
Office-Home	68.77	68.74	68.82	68.88	<b>68.99</b>	68.97	68.93	68.88	68.89	66.11

TABLE X: The relationships between inter-domain distributional alignment and intra-domain discriminative preservation (CSDA)

Task	IDDP	IDDA	IDDP+IDDA	Task	IDDP	IDDA	IDDP+IDDA	Task	IDDP	IDDA	IDDP+IDDA
U→M	54.95	<b>73.30</b>	73.40	M→U	75.50	<b>84.94</b>	85.72	C1→C2	91.39	<b>98.89</b>	100.0
C2→C1	90.69	<b>98.61</b>	99.44	Ms→Vo	<b>40.13</b>	35.49	40.52	Vo→Ms	<b>63.91</b>	57.92	63.99
C→A	<b>59.08</b>	55.22	61.38	C→W	<b>60.34</b>	58.31	61.36	C→D	55.41	<b>57.32</b>	57.96
A→C	<b>48.35</b>	44.43	47.64	A→W	<b>53.90</b>	52.88	55.59	A→D	<b>49.04</b>	47.77	52.23
W→C	37.85	<b>40.61</b>	41.23	W→A	33.61	<b>43.01</b>	45.41	W→D	93.63	<b>94.27</b>	94.90
D→C	36.24	<b>36.87</b>	37.93	D→A	39.67	<b>45.09</b>	47.29	D→W	<b>92.54</b>	92.20	93.56

TABLE XI: Accuracy (%) on the Office-Home dataset (OSDA, OS, OS\*, UNK) with varying  $\alpha_i$  values

Task(ResNet-50)	Metric	1.00	0.99	0.98	0.97	0.96	0.95	0.94	0.93	0.92	0.91	0.90
Ar→Cl	OS	71.8	70.2	<b>61.9</b>	55.7	46.1	38.9	35.2	30.7	26.8	23.0	19.7
	OS*	74.6	71.0	<b>61.3</b>	54.4	44.3	36.7	32.8	28.1	24.0	20.0	16.6
	UNK	0.00	49.1	<b>76.8</b>	87.1	91.9	94.1	95.3	96.2	96.9	98.0	98.6
Ar→Pr	OS	85.2	84.6	78.9	<b>74.3</b>	68.7	60.8	49.8	44.4	39.4	35.4	31.4
	OS*	88.6	86.1	79.2	<b>73.9</b>	67.9	59.5	48.0	42.3	37.0	32.9	28.7
	UNK	0.00	46.7	70.1	<b>83.8</b>	89.0	91.4	94.2	95.7	96.9	97.5	97.7
Cl→Pr	OS	77.5	78.1	<b>69.3</b>	65.6	61.3	56.0	49.8	43.7	37.4	33.0	29.9
	OS*	80.6	79.6	<b>69.3</b>	64.9	60.3	54.6	48.1	41.7	35.1	30.6	27.2
	UNK	0.00	42.3	<b>70.4</b>	82.0	87.6	90.3	91.9	93.1	94.2	95.3	96.0
Pr→Cl	OS	62.2	62.4	<b>54.3</b>	49.0	44.6	38.6	34.4	29.9	26.4	23.2	20.9
	OS*	64.7	63.1	<b>53.6</b>	47.8	43.0	36.6	32.2	27.5	23.8	20.4	18.0
	UNK	0.00	45.7	<b>72.0</b>	80.6	84.9	87.7	89.1	90.4	91.6	92.4	93.2
Rw→Cl	OS	68.7	69.1	63.8	<b>58.6</b>	51.5	46.9	42.8	39.2	36.5	34.1	30.8
	OS*	71.5	70.4	63.7	<b>57.8</b>	50.2	45.2	40.9	37.1	34.3	31.7	28.3
	UNK	0.00	35.8	67.8	<b>78.1</b>	84.3	88.4	91.1	92.2	92.9	93.8	94.6
Rw→Pr	OS	84.9	86.8	86.6	<b>85.9</b>	83.8	79.9	77.1	73.9	71.7	68.9	65.8
	OS*	88.3	88.7	87.7	<b>86.1</b>	83.7	79.5	76.5	73.1	70.7	67.8	64.6
	UNK	0.00	38.6	59.8	<b>80.9</b>	85.4	89.1	91.6	93.7	94.5	95.4	96.0

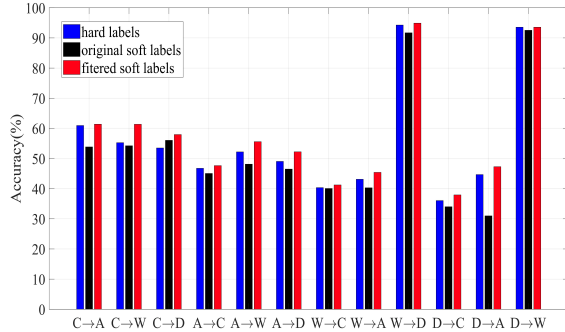


Fig. 5: Office31+Caltech256 dataset with different labels (CSDA)

best results are achieved with filtered soft labels compared with both hard labels and original soft labels. In addition, we also report the accuracies with varying numbers of the selected maximal probabilities in soft labels (*i.e.*, Table. IX), where the accuracy of each dataset is the average of all their tasks.

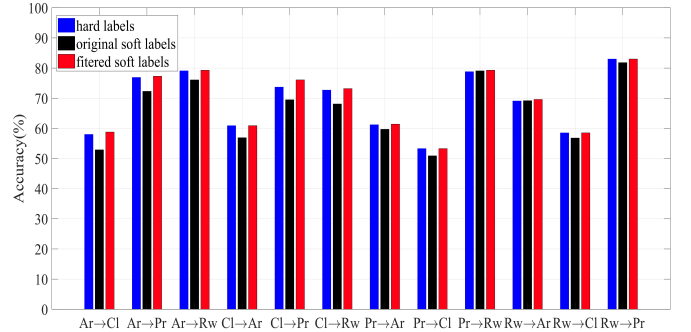


Fig. 6: Office-Home dataset with different labels (CSDA)

The results further validates the effectiveness of our filtering mechanism.

As mentioned before, the inter-domain distributional alignment (IDDA) and intra-domain discriminative preservation (IDDP) are of equal importance for the final knowledge transfer performance. As shown in Fig. 1 and Fig. 2, the per-

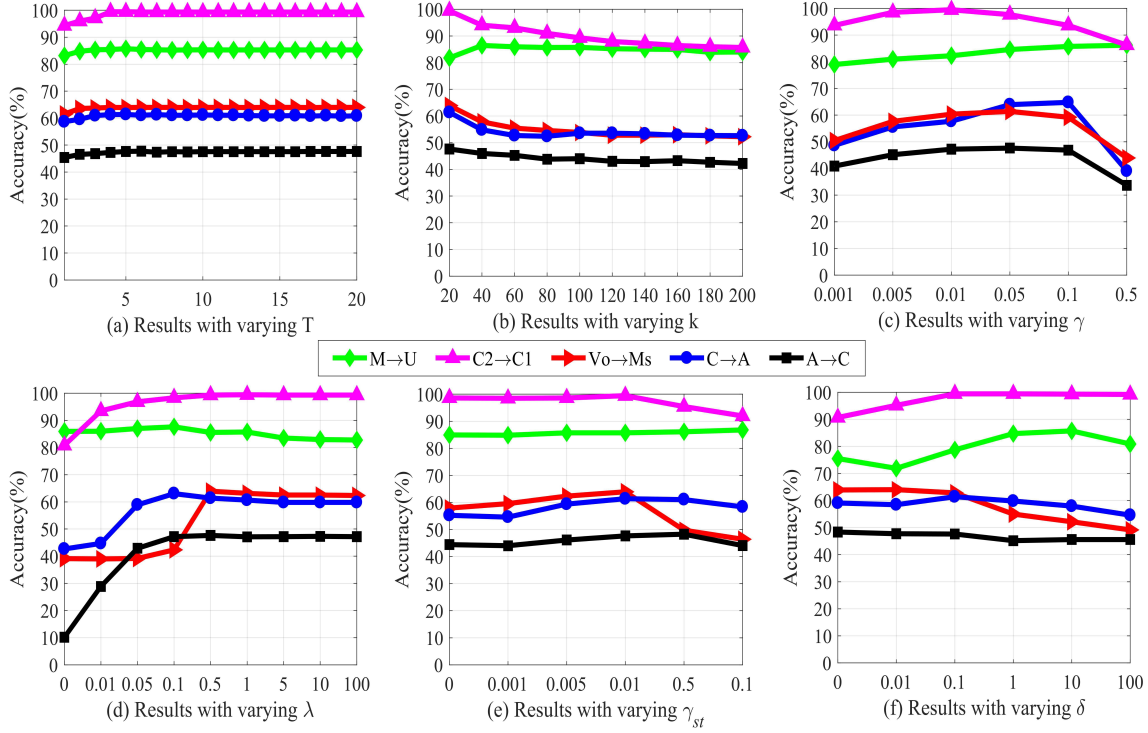


Fig. 7: Parameter sensitivity, the  $T$ ,  $k$ ,  $\gamma$ ,  $\lambda$ ,  $\gamma_{st}$  and  $\delta$  values in CSDA

formance on discriminative preservation is better than the distributional alignment on USPS+MNIST and COIL20 datasets while the opposite case is demonstrated on MSRC+VOC2007 dataset. Moreover, those two issues are getting more complicated on the Office31+Caltech256 dataset. Table. X reports their results on different tasks from USPS+MNIST, COIL20, MSRC+VOC2007 and Office31+Caltech256 datasets, and there are three circumstances corresponding to different considerations (*i.e.*, IDDP, IDDA, IDDP+IDDA). It is observed that the IDDA performs better than IDDP in the datasets of USPS+MNIST and COIL20, while worse than IDDP in MSRC+VOC2007 dataset. Furthermore, it is not sure which issue is the critical factor on Office31-Caltech256 dataset, while the best results are usually achieved by IDDP+IDDA. We notice that the experimental results agree with our observations, and it can be proved that both of them play important part contributing to final DA performance.

The parameters sensitivity are reported in Fig. 7, where 5 tasks from different datasets are adopted (*i.e.*,  $M \rightarrow U$ ,  $C2 \rightarrow C1$ ,  $Vo \rightarrow Ms$ ,  $C \rightarrow A$ ,  $A \rightarrow C$ ). Specifically, Fig. 7 (a) shows the convergence curve of our approach. We can see that the accuracy is monotonically increasing with the rise of iterations. The convergence curve becomes steady after about 5 iterations, which proves that our approach converges fast. Fig. 7 (b) shows the influence of the reduced dimensionality, it can be observed that the accuracies on the tasks  $C2 \rightarrow C1$ ,  $Vo \rightarrow Ms$ ,  $C \rightarrow A$  and  $A \rightarrow C$  are reduced slightly with the increase of  $k$ , while the accuracy on the task  $M \rightarrow U$  increased marginally. Fig. 7 (c) shows the effect of the regularization  $\gamma$ , we can see that the accuracies on the tasks  $C2 \rightarrow C1$ ,  $Vo \rightarrow Ms$ ,  $C \rightarrow A$  and  $A \rightarrow C$  reaches maximum and then decreases as the rise of  $\gamma$ , while the accuracy on the task  $M \rightarrow U$  maintains an increasing

trend. Moreover, the fixed optimal  $\gamma$ ,  $k$  values in this paper are small on the tasks  $C2 \rightarrow C1$ ,  $Vo \rightarrow Ms$ ,  $C \rightarrow A$  and  $A \rightarrow C$  but large on task  $M \rightarrow U$ . From these observations, we speculate that there exists a relationship between  $k$  and  $\gamma$ , and the value of  $\gamma$  should be larger with the rise of  $k$  since  $\gamma$  controls the scale of projections.

Fig. 7 (d) shows the impacts of subspace alignment, where the larger  $\lambda$  value corresponds to strong constraint that the source and target domain have to share a common space. It can be observed that the optimal results could be achieved in a small value, which plays an important role to further preserve some intra-domain data properties. Fig. 7 (e) and Fig. 7 (f) illustrate the influences of discriminative preservation and distributional alignment, which also indicates the relationships between these two issues. From Fig. 7 (e), we see that the discriminative preservation is not effective on the tasks  $C2 \rightarrow C1$  and  $M \rightarrow U$ , while it can boost the performance on the other three tasks. On the contrary, Fig. 7 (f) verifies that the distributional alignment promotes the results on the tasks  $C2 \rightarrow C1$  and  $M \rightarrow U$  greatly, while it has no effect on the other three tasks. Combining these observations with the results reported on Table. X, it further proves that the distributional reduction and discriminative preservation should be considered simultaneously due to the complicated practical applications.

From Table. XI, it is observed that the UNK accuracies are increased with decrease of  $\alpha_i$ , while the OS and OS\* reduced, because most samples are classified as the unknown classes. Therefore, we have to search an optimal  $\alpha_i$  to balance the OS, OS\* and the UNK accuracies. We can see that the good performance is achieved with either 0.98 or 0.99. Finally, through the analysis of those parameters, it proves that all of them can be tuned easily since they achieve the

optimal performance under a wide range and have interpretable physical meanings.

## V. CONCLUSION

In this paper, we proposed a novel approach for the challenges in both CSDA and OSDA scenarios, referred to as probabilistic filtered soft labels guided domain adaptation (PFSLG-DA). Our approach jointly reduces the inter-domain distributional differences and preserves the intra-domain data properties. As for the class-wise statistics in our model, not only the class-wise MMD is reformulated by the filtered soft labels, but also the class scatter matrix, where the small probabilities in soft labels are filtered out. In order to propagate the labels from the source domain to target domain correctly, a well-designed graph-based label propagation (GLP) is incorporated into the DA procedure, where the graph is getting more adaptive, the soft labels more accurate and the classification errors of source domain smaller. Remarkably, our approach could be easily extended to OSDA scenario using a refined GLP procedure, where the unknown classes in the target domain could be detected as accurately as possible, then the positive knowledge transfer could be achieved between the common classes of each domain. In the experiments, we not only proved that our approach is applicable for both CSDA and OSDA scenarios in an unsupervised manner, but also explored that if the shallow FDA approach can be used to reinforce deep features. The experimental results show that the soft labels with a well-designed filtering mechanism can further boost the positive knowledge transfer. Through the analysis of parameter  $\alpha_i$ , it was proved that the proposed approach not only detects the unknown classes in the target domain as accurately as possible, but also promotes the positive knowledge transfer between the shared classes of different domains.

## ACKNOWLEDGMENT

The authors would like to thank...

## REFERENCES

- [1] S. J. Pan and Q. Yang, "A survey on transfer learning," *IEEE TKDE*, vol. 22, no. 10, pp. 1345-1359, 2010.
- [2] Z. Ding, N. M. Nasrabadi and Y. Fu, "Semi-supervised deep domain adaptation via coupled neural networks," *IEEE TIP*, vol. 27, no. 11, pp. 5214-5224, 2018.
- [3] H. Lu, C. Shen, Z. Cao, Y. Xiao and A. V. D. Hengel, "An embarrassingly simple approach to visual domain adaptation," *IEEE TIP*, vol. 27, no. 7, pp. 3403-3417, 2018.
- [4] C. Hou, Y. H. Tsai, Y. Yeh and Y. F. Wang, "Unsupervised domain adaptation with label and structural consistency," *IEEE TIP*, vol. 25, no. 12, pp. 5552-5562, 2016.
- [5] S. Li, S. Song, G. Huang, Z. Ding and C. Wu, "Domain invariant and class discriminative feature learning for visual domain adaptation," *IEEE TIP*, vol. 27, no. 9, pp. 4260-4273, 2018.
- [6] J. Zhang, W. Li and P. Ogunbona, "Joint geometrical and statistical alignment for visual domain adaptation," in *CVPR*, 2017, pp. 5150-5158.
- [7] M. Long, J. Wang, G. Ding, J. Sun and P. S. Yun, "Transfer feature learning with joint distribution adaptation," in *ICCV*, 2013, pp. 2200-2207.
- [8] S. J. Pan, I. W. Tsang, J. T. Kwok and Q. Yang, "Domain adaptation via transfer component analysis," *IEEE TNN*, vol. 22, no. 2, pp. 199-210, 2011.
- [9] J. Tahmoresnezhad and S. Hashemi, "Visual domain adaptation via transfer feature learning," *KIS*, vol. 50, no. 2, pp. 585-605, 2017.
- [10] M. Ghifary, D. Balduzzi, W. B. Kleijn and M. Zhang, "Scatter component analysis: a unified framework for domain adaptation and domain generalization," *IEEE TPAMI*, vol. 39, no. 7, pp. 1414-1430, 2017.
- [11] Z. Ding, S. Li, M. Shao and Y. Fu, "Graph adaptive knowledge transfer for unsupervised domain adaptation," in *ECCV*, 2018, pp. 36-52.
- [12] F. Nie, S. Xiang, Y. Liu and C. Zhang, "A general graph-based semi-supervised learning with novel class discovery," *Neural Computing and Applications*, vol. 19, no. 4, pp. 549-555, 2010.
- [13] P. P. Busto and J. Gall, "Open set domain adaptation," in *ICCV*, 2017, pp. 754-763.
- [14] Z. Luo, Y. Zou, J. Hoffman and F. F. Li, "Label efficient learning of transferable representations across domains and tasks," in *NIPS*, 2017, pp. 164-176.
- [15] K. Saito, S. Yamamoto, Y. Ushiku and T. Harada, "Open set domain adaptation by backpropagation," in *ECCV*, 2018, pp. 156-171.
- [16] H. Liu, Z. Cao, M. Long, J. Wang and Q. Yang, "Separate to adapt: open set domain adaptation via progressive separation," in *CVPR*, 2019, pp. 2927-2936.
- [17] Y. Zhang, T. Liu, M. Long and M. I. Jordan, "Bridging theory and algorithm for domain adaptation," in *ICML*, 2019, pp. 7404-7413.
- [18] Y. Cao, M. Long and J. Wang, "Unsupervised domain adaptation with distribution matching machines," in *AAAI*, 2018, pp. 2795-2802.
- [19] L. Zhang, S. Wang, G. B. Huang, W. Zuo, J. Yang and D. Zhang, "Manifold criterion guided transfer learning via intermediate domain generation," arXiv preprint, 2019.
- [20] Z. Ding and Y. Fu, "Deep transfer low-rank coding for cross-domain learning," *IEEE TNNLS*, vol. 30, no. 6, pp. 1768-1779, 2019.
- [21] S. Motiian, M. Piccirilli, D. A. Adjeroh and G. Doretto, "Unified Deep Supervised Domain Adaptation and Generalization," in *ICCV*, 2017, pp. 5716-5726.
- [22] Z. Ding, N. M. Nasrabadi and Y. Fu, "Semi-supervised Deep Domain Adaptation via Coupled Neural Networks," *IEEE TIP*, vol. 27, no. 11, pp. 5214-5224, 2018.
- [23] Y. Ganin and V. S. Lempitsky, "Unsupervised domain adaptation by backpropagation," in *ICML*, 2015, pp. 1180-1189.
- [24] W. Hong, Z. Wang, M. Yang and J. Yuan, "Conditional generative adversarial network for structured domain adaptation," in *CVPR*, 2018, pp. 1335-1344.
- [25] Z. Pei, Z. Cao, M. Long and J. Wang, "Multi-adversarial domain adaptation," in *AAAI*, 2018, pp. 3934-3941.
- [26] J. Zhang, Z. Ding, W. Li, and P. Ogunbona, "Importance weighted adversarial nets for partial domain adaptation," in *CVPR*, 2018, pp. 8156-8164.
- [27] H. Shimodaira, "Improving predictive inference under covariate shift by weighting the log-likelihood function," *Statistical Planning and Inference*, vol. 90, no. 2, pp. 227-244, 2000.
- [28] A. Torralba and A. A. Efros, "Unbiased look at dataset bias," in *CVPR*, 2011, pp. 1521-1528.
- [29] B. Gholami, O. Rudovic and V. Pavlovic, "Punda: probabilistic unsupervised domain adaptation for knowledge transfer across visual categories," in *ICCV*, 2017, pp. 3601-3610.
- [30] M. Long, Y. Cao, J. Wang, and M. I. Jordan, "Learning transferable features with deep adaptation networks," in *ICML*, 2015, pp. 97-105.
- [31] M. Long, H. Zhu, J. Wang, and M. I. Jordan, "Deep transfer learning with joint adaptation networks," in *ICML*, 2017, pp. 2208-2217.
- [32] M. Long, J. Wang, G. Ding, J. Sun and P. S. Yu, "Transfer joint matching for unsupervised domain adaptation," in *CVPR*, 2014, pp. 1410-1417.
- [33] J. Wang, Y. Chen, S. Hao, W. Feng and Z. Shen, "Balanced distribution adaptation for transfer learning," in *ICDM*, 2017, pp. 1129-1134.
- [34] M. Long, G. Ding, J. Wang, J. Sun, Y. Guo and P. S. Yu, "Transfer sparse coding for robust image representation," in *CVPR*, 2013, pp. 407-414.
- [35] L. Zhang, W. Zuo and D. Zhang, "Lsd: latent sparse domain transfer learning for visual adaptation," *IEEE TIP*, vol. 25, no. 3, pp. 1177-1191, 2016.
- [36] M. Long, J. Wang, G. Ding, D. Shen and Q. Yang, "Transfer learning with graph co-regularization," *IEEE TKDE*, vol. 26, no. 7, pp. 1805-1818, 2014.
- [37] I. Redko and Y. Bennani, "Random subspaces NMF for unsupervised transfer learning," in *IJCNN*, 2014, pp. 3901-3908.
- [38] J. J. Y. Wang, Y. Sun and H. Bensmail, "Domain transfer nonnegative matrix factorization," in *IJCNN*, 2014, pp. 3605-3612.
- [39] I. H. Jhuo, D. Liu, D. T. Lee and S. F. Chang, "Robust visual domain adaptation with low-rank reconstruction," in *CVPR*, 2012, pp. 2168-2175.
- [40] M. Shao, D. Kit and Y. Fu, "Generalized transfer subspace learning through low-rank constraint," *IJCV*, vol. 109, no. 1-2, pp. 74-93, 2014.



- [41] S. Si, D. Tao and B. Geng, "Bregman divergence-based regularization for transfer subspace learning," *IEEE TKDE*, vol. 22, no. 7, pp. 929-942, 2010.
- [42] B. Gong, Y. Shi, F. Sha and K. Grauman, "Geodesic flow kernel for unsupervised domain adaptation," in *CVPR*, 2012, pp. 2066-2073.
- [43] A. Gretton, K. M. Borgwardt, M. J. Rasch, B. Schölkopf and A. J. Smola, "A kernel method for the two-sample-problem," in *NIPS*, 2006, pp. 513-520.
- [44] Y. Xu, X. Fang, J. Wu, X. Li, and D. Zhang, "Discriminative transfer subspace learning via low-rank and sparse representation," *IEEE TIP*, vol. 25, no. 2, pp. 850-863, 2016.
- [45] L. Luo, L. Chen, Y. Lu and S. Hu, "Discriminative label consistent domain adaptation," arXiv preprint, 2018.
- [46] H. Zhao, Z. Wang and F. Nie, "a new formulation of linear discriminant analysis for robust dimensionality reduction," *IEEE TKDE*, vol. 31, no. 4, pp. 629-640, 2019.
- [47] B. Fernando, A. Habrard, M. Sebban and T. Tuytelaars, "Unsupervised visual domain adaptation using subspace alignment," in *ICCV*, 2013, pp. 2960-2967.
- [48] B. Sun and K. Saenko, "Subspace distribution alignment for unsupervised domain adaptation," in *BMVC*, 2015, pp. 24.1-24.10.
- [49] F. Nie, S. Xiang, Y. Jia and C. Zhang, "Semi-supervised orthogonal discriminant analysis via label propagation," *Pattern Recognition*, vol. 42, no. 11, pp. 2615-2627, 2009.
- [50] Z. Ding and Y. Fu, "Robust transfer metric learning for image classification," *IEEE TIP*, vol. 26, no. 2, pp. 660-670, 2017.
- [51] A. Krizhevsky, I. Sutskever and G. E. Hinton, "ImageNet classification with deep convolutional neural networks," in *NIPS*, 2012, pp. 1106-1114.
- [52] K. He, X. Zhang, S. Ren, and J. Sun, "Deep residual learning for image recognition," in *CVPR*, 2016, pp. 770-778.
- [53] H. Venkateswara, J. Eusebio, S. Chakraborty and S. Panchanathan, "Deep hashing network for unsupervised domain adaptation," in *CVPR*, 2017, pp. 5385-5394.
- [54] Y. Ganin, E. Ustinova, H. Ajakan, P. Germain, H. Larochelle, F. Laviolette, M. Marchand, and V. Lempitsky, "Domain-adversarial training of neural networks," *JMLR*, vol. 17, no. 1, pp. 2096-2030, 2016.
- [55] M. Long, Z. Cao, J. Wang and M. I. Jordan, "Conditional adversarial domain adaptation," in *NIPS*, 2018, pp. 1647-1657.
- [56] A. Bendale and T. E. Boult, "Towards open set deep networks," in *CVPR*, 2016, pp. 1563-1572.
- [57] M. Long, H. Zhu, J. Wang and M. I. Jordan, "Unsupervised domain adaptation with residual transfer networks," in *NIPS*, 2016, pp. 136-144.



**Wei Wang** Biography text here.

**Zhihui Wang** Biography text here.

**Haojie Li** Biography text here.